Hydrol. Earth Syst. Sci., 30, 1261–1290, 2026
https://doi.org/10.5194/hess-30-1261-2026


Hydrology and Earth System Sciences
Open Access
EGU

# Synergistic impact of simultaneously assimilating radar- and radiometer-based soil moisture retrievals on the performance of numerical weather prediction systems

**Yonghwan Kwon[1], Sanghee Jun[1], Hyunglok Kim[2], Kyung-Hee Seol[1], In-Hyuk Kwon[1], Eunkyu Kim[1], and Sujeong Cho[1]**

[1]Korea Institute of Atmospheric Prediction Systems, Seoul 07071, South Korea
[2]Department of Environment and Energy Engineering, Gwangju Institute of Science and Technology (GIST), Gwangju 61005, South Korea

**Correspondence:** Yonghwan Kwon (yhkwon@kiaps.org)

Received: 13 March 2025 – Discussion started: 30 April 2025
Revised: 10 October 2025 – Accepted: 11 February 2026 – Published: 3 March 2026

**Abstract.** The combined use of independent soil moisture data from radar and radiometer measurements in data assimilation (DA) systems is expected to yield synergistic performance gains due to their complementary strengths. This study evaluates the impact of simultaneously assimilating soil moisture retrievals from ASCAT (Advanced SCATterometer) and SMAP (Soil Moisture Active Passive) into the Korean Integrated Model (KIM) using a weakly coupled DA framework based on the National Aeronautics and Space Administration's Land Information System (LIS). The Noah land surface model (LSM) within LIS, which is the same as that used in KIM, is used to simulate land surface states and assimilate soil moisture retrievals. The impact of soil moisture DA is evaluated using independent reference datasets, assessing its influence on soil moisture analysis and numerical weather prediction performance. Overall, assimilating single-sensor soil moisture data, ASCAT or SMAP, into the LSM improves global soil moisture analysis accuracy by 4.0 % and 10.5 %, respectively, compared to the control case without soil moisture DA, achieving the most significant enhancements in croplands. Relative to single-sensor soil moisture DA, multi-sensor soil moisture DA yields more balanced skill enhancements for both specific humidity and air temperature analyses and forecasts. The most pronounced synergistic improvements by simultaneously assimilating both soil moisture products are observed in the 2 m air temperature analysis and forecast, especially when both soil moisture products have a positive impact. Precipitation forecast skill also improves with multi-sensor soil moisture DA, although the improvements are not consistent across regions and events. This paper discusses remaining issues for future studies to further improve the weather prediction performance of the KIM-LIS multi-sensor soil moisture DA system.

## 1 Introduction

Soil moisture is one of the decisive land surface state variables that control land-atmosphere interactions associated with water and energy cycles (Gentine et al., 2011; Koster et al., 2004; Tuttle and Salvucci, 2016) and that determine surface water infiltration, percolation, and runoff (Assouline, 2013; Orth and Seneviratne, 2013). Many studies underline the importance of accurate knowledge of the spatial and temporal soil moisture variability for various hydrometeorological applications (e.g., Jalilvand et al., 2019; Shin and Jung, 2014; Wanders et al., 2014; Yuan et al., 2011). Because of the long memory effect of soil moisture, proper soil moisture initialization is a prominent part of numerical weather prediction (NWP), particularly in the lower atmosphere (Dirmeyer and Halder, 2016; Drusch and Viterbo, 2007; Jun et al., 2021; Koster et al., 2010; Kwon et al., 2024; van den Hurk et al., 2012).

As a viable method to produce spatially and temporally complete, observation-constrained estimates of soil moisture

profiles (Bolten et al., 2010; Reichle et al., 2002a), assimilating satellite-based soil moisture data into land surface models (LSMs) has been widely explored. Soil moisture data assimilation (DA) optimally merges remotely-sensed near-surface soil moisture observations with modeled soil moisture estimates based on their respective uncertainties (Kumar et al., 2008a; Reichle et al., 2008), and it can generate soil moisture estimates superior to either observations or models alone when the relative size of the uncertainties is properly characterized (Liu et al., 2011; Blyverket et al., 2019). A number of studies have applied soil moisture DA to improve flood and drought forecasts (e.g., Azimi et al., 2020; Gavahi et al., 2022; Laiolo et al., 2016), streamflow and runoff predictions (e.g., Baugh et al., 2020; Brocca et al., 2010; Lievens et al., 2016), irrigation characterization (e.g., Kwon et al., 2022; Nair and Indu, 2019), and evaporative flux estimates (e.g., Li et al., 2020; Pipunic et al., 2013). In particular, it has been demonstrated that the assimilation of satellite-based soil moisture retrievals into LSMs that are coupled to atmospheric models has a positive impact on weather forecast skill (e.g., Draper and Reichle, 2019; Jun et al., 2021; Kwon et al., 2024; Lin and Pu, 2020; Lodh et al., 2022; Yin et al., 2019).

In addition to DA methods, a variety of alternative data fusion techniques have been widely explored to integrate soil moisture information from different sources, including remote sensing products, in-situ measurements, model simulations, and reanalysis datasets. One group of approaches relies on statistical methods (e.g., Min et al., 2022; Wang et al., 2021; Xie et al., 2022), such as unweighted averaging, linear weight fusion, and emergent constraint. Another group leverages machine learning (e.g., Huang et al., 2023; Lamichhane et al., 2025; Long et al., 2019; Zhang et al., 2022, Zeng et al., 2024) and deep learning techniques (e.g., Fuentes et al., 2022; Huang et al., 2022; Jiang et al., 2025; Singh and Gaurav, 2023; van der Schalie et al., 2018). These machine learning and deep learning approaches are rapidly gaining prominence because of their ability to incorporate diverse data sources and to capture complex, nonlinear relationships between datasets (Huang et al., 2022; Zeng et al., 2024). While different fusion approaches have distinct strengths and limitations, this study is devoted to DA methods, with the goal of improving model-based soil moisture estimates that interact with atmospheric processes in operational land-atmosphere coupled systems, thereby enhancing weather forecasts.

Microwave satellite systems provide useful information to retrieve surface soil moisture data at the global scale owing to their sensitivity to soil dielectric properties that mainly depend on soil water content and surface roughness (Schmugge et al., 1986). Many satellite soil moisture products have been generated from microwave observations at different frequencies (i.e., X, C and L-band) using various retrieval algorithms in different systems during the past several decades (Kumar et al., 2019; Nair and Indu, 2018). Among them, the Advanced SCATterometer (ASCAT) (e.g., Bartalis et al., 2007; Wagner et al., 2013), Soil Moisture Active Passive (SMAP) (e.g., Chan et al., 2018; O'Neill et al., 2023), and Soil Moisture and Ocean Salinity (SMOS) (e.g., Kerr et al., 2012) are relatively modern sensors that have been widely used in soil moisture DA studies (e.g., Blyverket et al., 2019; Jun et al., 2021; Khaki and Awange, 2019; Kolassa et al., 2017; Kumar et al., 2019; Kwon et al., 2022, 2024; Nair and Indu, 2019; Renzullo et al., 2014; Seo et al., 2021; Tangdamrongsub et al., 2020). In addition, most recently, Nguyen et al. (2025) have demonstrated the usefulness of soil moisture retrievals based on signals from the Global Navigation Satellite Systems. Kumar et al. (2019) report that soil moisture retrievals from these modern sensors exhibit better performance in DA systems than those from older sensors.

The present study focuses on the use of the ASCAT and SMAP soil moisture products to improve modeled soil moisture estimates via assimilation. The ASCAT soil moisture product is generated from active microwave backscatter measurements at C-band (5.3 GHz) while the SMAP soil moisture data is based on passive microwave satellite systems, which utilize naturally emitted brightness temperature from the Earth's surface at an L-band (1.4 GHz) frequency. The C-band (i.e., ASCAT) and L-band (i.e., SMAP) sensors typically provide soil moisture information for soil depth of 0–2 and 0–5 cm, respectively (Kim et al., 2018). Compared to passive radiometers, radar observations (i.e., ASCAT) have smaller footprint sizes (i.e., finer spatial resolutions) and thus provide better spatial details of soil moisture (Nair and Indu, 2019). However, ASCAT has large uncertainties over regions of complex topography due to multiple scattering effects (Dobson and Ulaby, 1986). In contrast, radiometer (SMAP) observations are more sensitive to the presence of soil moisture than active radars (Kolassa et al., 2017), but the accuracy of their soil moisture products is strongly influenced by vegetation water content and surface temperature (Paloscia and Pampaloni, 1988).

Because of their complementary advantages, better soil moisture estimates can be obtained by assimilating the soil moisture data from multiple sources into the model-simulated soil moisture within a DA system. There have been some efforts to synergistically combine multiple active and passive observations for spatially and temporally improved soil moisture retrievals such as the European Space Agency Climate Change Initiative (ESA CCI, Dorigo et al., 2017). In addition, one of the key goals of the SMAP mission was to utilize both active and passive sensors on the same satellite platform to retrieve high spatial resolution global near-surface soil moisture data with great accuracy (Entekhabi et al., 2010). However, due to mechanical malfunction of the SMAP radar, alternative radar observations from other satellites (e.g., Sentinel-1) have been combined with the SMAP radiometer data to maintain data continuity (Das et al., 2019). Meanwhile, Kolassa et al. (2017) and Nair and Indu (2019) demonstrate that simultaneously assimilating individual radar- and radiometer-based soil moisture retrievals achieves comparable overall performance to the assimilation

of the blended (i.e., radar + radiometer) soil moisture products. In this study, we do not aim to retrieve or assimilate blended soil moisture products from multiple satellite measurements. Instead, we independently utilize soil moisture data from each sensor (i.e., ASCAT and SMAP) within a land-atmosphere coupled DA system, while also incorporating both observations separately rather than combining them spatially. This approach may provide a more effective way to account for the relative reliability of each sensor in soil moisture assimilation (Kolassa et al., 2017), and offers greater flexibility for assimilating various soil moisture products simultaneously in different combinations.

This study is built on a land-atmosphere coupled DA system, which consists of the Korean Integrated Model (KIM; Hong et al., 2018) and the National Aeronautics and Space Administration (NASA) Land Information System (LIS; Kumar et al., 2006, 2008b; Peters-Lidard et al., 2007). Hereafter, this system is referred to as the KIM-LIS coupled system. As an operational global NWP model at the Korea Meteorological Administration, KIM has been developed by the Korea Institute of Atmospheric Prediction Systems (KIAPS). KIM has capabilities of conducting short-to-medium-range and extended-range weather forecasts, and of implementing atmospheric DA to generate improved atmospheric initial conditions for the forecasts (Kwon et al., 2018). Land DA in the current Korea Meteorological Administration's operational NWP system is based on the KIM-LIS coupled system and ingests the ASCAT soil moisture retrievals to constrain the modeled soil moisture (Jun et al., 2021). Recently Kwon et al. (2024) have demonstrated the feasibility of assimilating the SMAP soil moisture retrievals into the Noah LSM (Ek et al., 2003) within the KIM-LIS system to enhance the global soil moisture estimates and weather forecast performance of KIM.

While several studies have explored the simultaneous use of radar and radiometer-based soil moisture data in offline land DA systems, mainly to improve soil moisture estimates and associated hydrological processes (e.g., Draper et al., 2012; Khaki and Awange, 2019; Khaki et al., 2019, 2020; Kolassa et al., 2017; Kumar et al., 2019; Nair and Indu, 2019; Renzullo et al., 2014; Seo et al., 2021; Tangdamrongsub et al., 2020), only a few have investigated their impacts on atmospheric forecasts in land-atmosphere coupled NWP systems (e.g., de Rosnay et al., 2022; Draper and Reichle, 2019; Fairbairn et al., 2024). Even among studies using coupled forecast systems, most assimilate only ASCAT and SMOS together, despite evidence that SMAP provides high-quality soil moisture data (e.g., Bhuiyan et al., 2018; Chan et al., 2018; Colliander et al., 2017) and often outperforms other sensors (Kumar et al., 2018). In this regard, the novelty of this study is the combined use of ASCAT and SMAP soil moisture products in the KIM-LIS-based land-atmosphere coupled DA system, demonstrating their feasibility.

The present study aims to evaluate the relative (individual) and combined performance of C-band radar-based (i.e., ASCAT) and L-band radiometer-based (i.e., SMAP) surface soil moisture products in improving the global soil moisture analysis and atmospheric analysis/forecast via assimilation within the KIM-LIS coupled system. We first assimilate each soil moisture product individually into the Noah LSM in the KIM-LIS system over the global domain, and compare their respective performance gains. The synergistic impacts of simultaneously assimilating the ASCAT and SMAP soil moisture retrievals on the global estimates of lower atmospheric variables are then investigated.

## 2 KIM-LIS-based weakly coupled DA system

The KIM-LIS system (Jun et al., 2021; Kwon et al., 2024) is a weakly coupled DA system, in which the land analysis and atmospheric analysis are implemented independently (Fig. 1). The present study uses the KIM version 3.9 and LIS version 7.4, the same versions as those used in Kwon et al. (2024). KIM (Hong et al., 2018) is composed of a global non-hydrostatic dynamical core using a cubed-sphere grid system with up to 91 vertical levels on a hybrid-sigma coordinate system (Song et al., 2017; Kwon et al., 2018). LIS (Kumar et al., 2006, 2008b; Peters-Lidard et al., 2007) is a land surface hydrological modeling and DA system where various LSMs, DA schemes, and surface coordinate systems are available for different applications. In this study, the latitude-longitude grid system is used for LIS.

KIM and LIS employ separate versions of the Noah LSM, referred to as KIM-LSM and LIS-LSM, respectively, in Fig. 1 to simulate land-surface hydrological processes. In the Noah LSM (Ek et al., 2003), a soil column (2 m total depth) is discretized into four layers with the standard thickness of 0.1, 0.3, 0.6, and 1.0 m from surface to bottom for estimation of soil moisture and soil temperature. The original Noah version of KIM-LIS is 2.7.1, but it has undergone many updates based on later versions of the Noah LSM with additional modifications to physical parameterizations and land surface inputs to achieve optimal performance of KIM (Koo et al., 2017). As in Jun et al. (2021) and Kwon et al. (2024), the Noah LSM version 3.3 implemented within LIS is used for LIS-LSM by applying the same modifications to ensure consistency between KIM-LSM and LIS-LSM.

The KIM-LIS coupled system conducts a analysis/forecast cycle every 6 h [i.e., 00:00, 06:00, 12:00, and 18:00 Coordinated Universal Time (UTC) cycles] where KIM and LIS run for time windows of 12 h (i.e., −3 to +9 h) and 6 h (i.e., −6 to 0 h), respectively, as outlined in Fig. 1. LIS-LSM (i.e., Noah LSM) creates an ensemble of background (prior) soil moisture estimates forced by atmospheric fields from the previous UTC cycle (0 to +6 h) KIM analysis/-forecast, which are remapped from the cubed-sphere grid to the latitude-longitude grid and perturbed by adding Gaussian random perturbations. Additional random perturbations are imposed on the prior soil moisture estimates, which are then

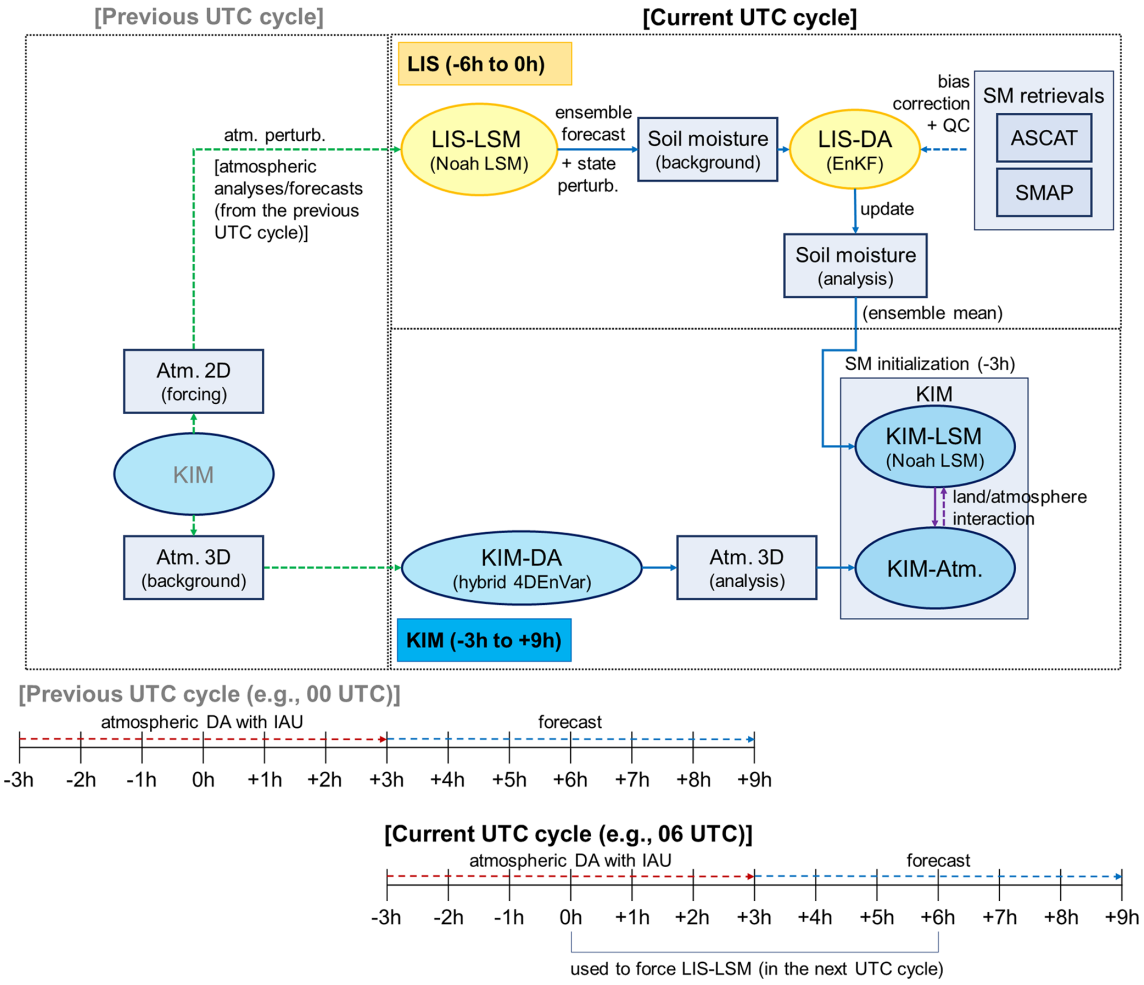


**Figure 1.** Schematic diagram of the KIM-LIS-based land-atmosphere weakly coupled data assimilation (DA) system. The figure outlines the process flow between KIM and LIS in one UTC cycle that is performed four times (i.e., 00:00, 06:00, 12:00, and 18:00 UTC cycles) a day (IAU: incremental analysis update, QC: quality control).

merged with remotely-sensed soil moisture retrievals using the ensemble Kalman filter (EnKF) method (Evensen, 1994; Reichle et al., 2002b) to generate the soil moisture analysis. This sequential EnKF procedure (i.e., soil moisture forecast and analysis) is performed from −6 to 0 h in the current UTC cycle. LIS writes land outputs every 3 h (i.e., at −3 and 0 h) and generates a restart file at 0 h. The restart file contains the complete set of model state variables at that time, enabling LIS-LSM to be consistently re-initialized in the subsequent UTC cycle. The soil moisture analysis from LIS at −3 h is remapped from the latitude-longitude grid to the cubed-sphere grid, and is used to initialize the soil moisture conditions of KIM-LSM that provides land boundary conditions for the KIM analysis and forecast from −3 to +9 h in the current UTC cycle. The atmospheric analysis is performed based on the hybrid four-dimensional ensemble variational (hybrid 4DEnVar) DA method (Song et al., 2017; Kwon et al., 2018). To minimize the initialization shock resulting from the atmospheric DA, the four-dimensional incremental analysis update (4DIAU; Lorenc et al., 2015) is employed within an atmospheric assimilation window (i.e., −3 to + 3h). KIM is further run without DA until +9 h, and the KIM analyses/forecasts from 0 to +6 h in the current UTC cycle are then used for the next UTC cycle LIS implementation.

Although the remapping procedures required to share information between KIM and LIS may introduce some error, Jun et al. (2021) and Kwon et al. (2024) have demonstrated that soil moisture DA based on the KIM-LIS system provides beneficial impacts on improving the weather forecast performance of KIM. In addition, the KIM-LIS coupled system, which employs the LIS-based land DA, has several advantages: (1) it can readily leverage the existing land DA functions of LIS, and (2) it allows straightforward implementation of new land DA developments due to LIS's extensible framework.

## 3 Satellite-based soil moisture retrievals

We assimilate the satellite-based near-surface soil moisture retrievals from ASCAT and SMAP individually and together into the Noah LSM to constrain the modeled soil moisture estimates. A brief explanation of the soil moisture products is given below.

### 3.1 Active soil moisture product: ASCAT

ASCAT is a real aperture radar onboard the Meteorological Operational (MetOp) satellites (i.e., MetOp-A, MetOp-B, and MetOp-C), and measures radar backscatter at C-band (5.3 GHz) VV (vertical transmit vertical receive) polarization (Wagner et al., 2013). The equator crossing times of the MetOp satellites are 09:30 am/pm local solar time (LST) for the descending and ascending overpasses, respectively, with a revisit frequency of 1–3 d. The ASCAT soil moisture is retrieved based on the Vienna University of Technology (TU Wien) change detection algorithm (Wagner et al., 1999, 2010), and provides an estimate of the degree of water saturation (ranging between 0 % and 100 %) of the top 0–2 cm soil layer.

We use the MetOp-B/C ASCAT near-real time soil moisture product at 12.5 km swath grid. The soil moisture product used in this study was obtained directly from the European Organisation for the Exploitation of Meteorological Satellites (EUMETSAT) for use in the Korea Meteorological Administration's operational weather prediction system while the same product can be downloaded from the EUMETSAT Earth Observation Portal (https://data.eumetsat.int/product/EO:EUM:DAT:METOP:SOMO12, last access: 23 February 2026).

### 3.2 Passive soil moisture product: SMAP

The SMAP mission provides volumetric soil moisture ($m^3\ m^{-3}$) for the top 0–5 cm of the soil, derived from L-band (1.4 GHz) passive microwave radiometer measurements (Entekhabi et al., 2010). It has a revisit cycle of 2–3 d, with local equator-crossing times of 6 am (descending) and 6 pm (ascending).

The present study uses the SMAP Level 2 (L2) Radiometer Half-Orbit 36 km Equal Area Scalable Earth (EASE)–Grid soil moisture data (SPL2SMP version 9, O'Neill et al., 2023), which is obtained from the National Snow and Ice Data Center (NSIDC, https://doi.org/10.5067/K7Y2D8QQVZ4L, O'Neill et al., 2023). The SMAP soil moisture retrievals based on the Dual Channel Algorithm (DCA, Chaubell et al., 2020) are assimilated.

### 3.3 Bias correction of the soil moisture data

Typical DA algorithms are designed to correct random errors under the assumption of unbiased state estimates between models and observations (Dee and Da Silva, 1998). However, there are generally large systematic discrepancies between modeled and satellite-retrieved soil moisture because of their different representations of soil moisture associated with the geophysical definition and horizontal/vertical scales (Koster et al., 2009; Kumar et al., 2019). Therefore, soil moisture DA systems essentially employ appropriate bias correction strategies to remove these systematic biases prior to assimilation, and thus to comply with the DA assumption of unbiased models and observations (Kolassa et al., 2017; Reichle and Koster, 2004). In this study, bias correction is implemented differently for the ASCAT and SMAP soil moisture products. That is, we apply cumulative distribution function (CDF) matching (Reichle and Koster, 2004) and anomaly correction methods (Kwon et al., 2022) to assimilate the ASCAT and SMAP soil moisture retrievals, respectively, into the Noah LSM within the KIM-LIS coupled system. The use of the anomaly correction method for SMAP follows our previous investigations (Kwon et al., 2022, 2024) aiming to minimize the loss of useful information from the original data through bias correction. In contrast, traditional CDF matching is applied to ASCAT, since the anomaly correction method is not applicable due to differences in soil moisture data types between ASCAT (soil wetness index) and the model (volumetric soil moisture in $m^3\ m^{-3}$). Further details are provided in the following two paragraphs.

The CDF matching is a commonly used bias correction method in soil moisture DA. Through the CDF matching, in this study, the ASCAT soil wetness index data are transformed to volumetric soil moisture ($m^3\ m^{-3}$) by correcting all the statistical moments of the original ASCAT data to those of the Noah-simulated soil moisture. Existing soil moisture DA studies use two different CDF matching approaches. One uses a lumped CDF computed using all seasons data (i.e., pixel-wise single CDF for each data type) (e.g., Draper et al., 2011, 2012; Kumar et al., 2009, 2014; Reichle et al., 2007) while the other uses monthly-stratified CDFs (i.e., pixel-wise 12 CDFs for each data type) (e.g., Jun et al., 2021; Kumar et al., 2015; Kwon et al., 2022, 2024; Santanello et al., 2016). Kumar et al. (2015) and Santanello et al. (2016) suggest using the monthly CDF rather than the lumped CDF to mitigate spurious statistical artifacts in the bias-corrected soil moisture by the CDF matching. Kwon et al. (2024) show that abnormal fluctuations are witnessed in the lumped CDF-based rescaled soil moisture, particularly in dry periods, and Kwon et al. (2022) demonstrate that soil moisture DA employing the monthly CDF achieves better soil moisture analysis than that applying the lumped CDF matching. Based on these previous findings, we implement the monthly CDF matching for the ASCAT soil moisture DA.

The anomaly correction method, proposed by Kwon et al. (2022), is a simpler alternative to traditional bias correction approaches. It aims to reduce the reliance of DA systems on rescaling methods like the CDF matching, which is known to cause significant information loss in the original soil moisture data, especially when human-induced pro-

cesses (e.g., irrigation activities), poorly represented in models, are the dominant source of systematic discrepancies between observations and models (Kumar et al., 2015; Nearing et al., 2018). Instead of rescaling the SMAP soil moisture retrievals, the anomaly correction approach obtains the soil moisture temporal variability (i.e., anomaly) information by subtracting the long-term soil moisture mean from the original SMAP data. The extracted SMAP soil moisture anomaly is added to the long-term mean of the modeled soil moisture, which is then assimilated into the LSM. The anomaly correction assumes that the systematic bias between observations and models is dominated by the climatological mean difference and higher moment (e.g., standard deviation) differences are negligible. Kwon et al. (2022) and Kwon et al. (2024) demonstrate that the SMAP soil moisture data and Noah-simulated soil moisture satisfy this underlying assumption over the continental United States and global domain, respectively. In particular, Kwon et al. (2024) show that the anomaly correction-based SMAP soil moisture DA is effective in improving the global soil moisture estimates and weather forecast skill of the KIM-LIS coupled system that employs the Noah LSM.

### 3.4 Quality control of the soil moisture data

The ASCAT and SMAP soil moisture retrievals undergo quality control before DA by removing inaccurate or uncertain soil moisture observations based on strategies employed in previous soil moisture DA studies (e.g., Blyverket et al., 2019; Draper et al., 2012; Ferguson et al., 2020; Jun et al., 2021; Kolassa et al., 2017; Kumar et al., 2014, 2019; Kwon et al., 2022, 2024; Nair and Indu, 2019). Firstly, before bias correction, the soil moisture data are discarded when the data quality flags provided with each soil moisture product indicate that the data accuracy is impacted by open water bodies, dense vegetation, urban areas, precipitation, snow cover, frozen ground, complex topography, or anthropogenic Radio Frequency Interference (RFI). Especially, the ASCAT soil moisture retrievals are assimilated only when the Estimated Soil Moisture Error (ESME) is less than 16 %, and the topographic complexity and wetland fraction are below 20 % and 15 %, respectively, as applied in Jun et al. (2021). These uncertainty thresholds are slightly higher than those used in Draper et al. (2012) and Kolassa et al. (2017) for the purpose of utilizing more data in a near-real time operational DA system.

Secondly, the model-based quality control is additionally applied to both ASCAT and SMAP after bias correction. Specifically, assimilation of ASCAT and SMAP soil moisture into the Noah LSM is not performed in the case that (1) model background estimates indicate active precipitation events or frozen/snow-covered soil conditions, that (2) the model land cover type and green vegetation fraction inputs from the Moderate resolution imaging spectroradiometer (MODIS) International Geosphere-Biosphere Programme (IGBP) data (Friedl et al., 2002) and the National Centers for Environmental Prediction (NCEP), respectively, indicate that a grid cell is classified as forests or has green vegetation fraction greater than 0.7, or that (3) bias-corrected soil moisture retrievals are close to wilting point or saturation.

## 4 DA methods

### 4.1 Atmospheric DA

Atmospheric DA in KIM is based on a hybrid four-dimensional ensemble variational (hybrid 4DEnVar) DA method as described in Kwon et al. (2018) and Song et al. (2017). In this study, we assimilate both conventional and non-conventional atmospheric data including the Advanced Microwave Sounding Unit-A (AMSU-A), Atmospheric Motion Vectors (AMVs), Microwave Humidity Sounder (MHS), Global Positioning System Radio Occultation (GPS-RO), Infrared Atmosphere Sounding Interferometer (IASI), Advanced Technology Microwave Sounder (ATMS), Cross-track Infrared Sounder (CrIS), and observations obtained from surface, aircraft, and sonde. The KIM Package of Observation Processing (KPOP, Kang et al., 2019) is employed to preprocess (e.g., quality control and bias correction) the observations before assimilation. Details of the KIM hybrid 4DEnVar DA scheme are provided in Sect. S1 of the Supplementary Material and in Kwon et al. (2018) and Song et al. (2017).

### 4.2 Land soil moisture DA

In the KIM-LIS coupled system, land DA is conducted by the LIS-DA subsystem (Fig. 1) in which various DA schemes are available. The current study applies a 1-dimensional EnKF method (Reichle et al., 2002b) to assimilate satellite soil moisture retrievals (i.e., ASCAT and SMAP) into the Noah LSM. The EnKF is one of the widely used DA schemes for nonlinear hydrological applications (e.g., Cho et al., 2023; Crow and Van den Berg, 2010; Draper and Reichle, 2019; Kim et al., 2021a; Kwon et al., 2019, 2021; Reichle et al., 2023; Renzullo et al., 2014; Xu et al., 2021) because of its relatively flexible and computationally efficient nature (Keppenne, 2000).

Within the EnKF-based DA system, model forecasts and analysis updates are performed alternately. That is, the ensemble forecasts of model prognostic state variables are propagated forward in time until observations are available, and the forecasted states are updated in the assimilation step when and where observations exist. The resulting analysis ensemble is then used as the initial condition for the next model forecast. In this study, the control vectors that are directly updated by assimilating the ASCAT and SMAP soil moisture retrievals include the Noah LSM estimates of soil moisture at four soil layers while other related hydrometeorological variables are adjusted through model physics

in subsequent model integrations. As we conduct the 1-dimensional EnKF, the soil moisture analysis in a given grid is produced independently of neighboring grids.

The EnKF increments are determined depending on the relative uncertainties (error variances) of model and observation. The model uncertainty (background error covariance) is represented by the ensemble forecast spread (ensemble size of 20), which is obtained at each grid by randomly perturbing the atmospheric variables from KIM including shortwave radiation, longwave radiation, and precipitation, and by additionally (randomly) perturbing the Noah LSM-simulated soil moisture estimates. Shortwave radiation and precipitation are perturbed by applying log-normally distributed multiplicative perturbations with standard deviations of 0.3 and 0.5, respectively, while normally distributed additive perturbations are applied to longwave radiation (with a standard deviation of 50 $W\,m^{-2}$) and the soil moisture (SM) estimates at four soil layers [with standard deviations of 0.01, 0.006, 0.003, and 0.0015 $m^3\,m^{-3}$ for SM1 (top layer), SM2, SM3, and SM4 (bottom layer), respectively]. First-order autoregressive temporal correlations and cross-variable correlations are also considered during the perturbation (Table 1), whereas horizontal error correlations are neglected. The perturbation parameters used in this study are determined based on Kumar et al. (2017, 2019) and Reichle et al. (2008), and have also been effectively applied in Jun et al. (2021) and Kwon et al. (2024).

The spatially and temporally constant observation error standard deviations of 10 % and 0.02 $m^3\,m^{-3}$ are applied for ASCAT and SMAP soil moisture retrievals, respectively, based on previous DA studies (e.g., Dorigo et al., 2010; Draper et al., 2012; Ferguson et al., 2020; Kolassa et al., 2017; Kwon et al., 2022, 2024). In the KIM-LIS coupled system, the ASCAT-derived soil wetness index data are scaled into the Noah LSM soil moisture climatology (in $m^3\,m^{-3}$) through the CDF matching (see Sect. 3.3) to remove the systematic bias between the ASCAT soil moisture and Noah-simulated soil moisture. Correspondingly the 10 % ASCAT soil moisture error standard deviation is also locally scaled by the ratio of the Noah LSM and ASCAT soil moisture time series standard deviations following Draper et al. (2012) and Jun et al. (2021). Unlike ASCAT, the SMAP soil moisture data are provided in the same unit as the Noah LSM soil moisture, and only the climatological mean biases between the SMAP soil moisture and modeled soil moisture are corrected during the bias correction procedure (see Sect. 3.3). Therefore, the observation error standard deviation of SMAP is not scaled in this study.

Note that there is a mismatch in the surface soil layer depth between the soil moisture observations (i.e., 0–2 cm for ASCAT and 0–5 cm for SMAP) and Noah LSM (i.e., 0–10 cm). However, Shellito et al. (2016, 2018) and Nair and Indu (2019) have demonstrated that changing the surface layer depth in the model from 10 to 2 cm or 5 cm has only a marginal impact on the simulated soil moisture. Moreover, because we apply the systematic bias correction of the soil moisture retrievals before assimilation, the impact of the surface soil layer depth difference on the DA performance is assumed to be negligible.

## 5 Experiments

Land-atmosphere coupled DA experiments (with a 6 h cycling frequency) using the active radar (i.e., ASCAT) and passive radiometer (i.e., SMAP) soil moisture retrievals are designed as summarized in Table 2. CTL, a control case serving as a baseline experiment, only assimilates atmospheric observations while an open-loop ensemble simulation of the Noah LSM is performed without soil moisture assimilation. SG_AT and SG_SP are single-sensor soil moisture DA experiments where the near-surface soil moisture data from individual sensors (ASCAT or SMAP, respectively) are assimilated into the Noah LSM using the 1-dimensional EnKF with an ensemble size of 20. MT_ATSP, a multi-sensor soil moisture DA experiment, jointly assimilates both ASCAT and SMAP soil moisture products to investigate the synergistic impact of assimilating the radar- and radiometer-based soil moisture retrievals together on improving the atmospheric analysis/forecast of the KIM-LIS coupled system. As explained in Sect. 3.3, the CDF matching and anomaly correction methods are applied for bias correction of the ASCAT and SMAP soil moisture retrievals, respectively, in the single- and multi-sensor soil moisture DA experiments. Atmospheric DA is performed identically in all experiments.

This study uses the same model setup and experimental period as in Kwon et al. (2024). We use the Shuttle Radar Topography Mission (SRTM) elevation (Farr et al., 2007), MODIS-IGBP land cover (Friedl et al., 2002), National Centers for Environmental Prediction (NCEP) green vegetation fraction and surface albedo, and the blended State Soil Geographic (STATSGO, Miller and White, 1998)/Food and Agriculture Organization (FAO) soil texture (Reynolds et al., 2000) as land inputs for the Noah LSM. The LSM and KIM deterministic component are run over the global domain at a horizontal resolution of 25 km while the KIM ensemble component is run at a 50 km horizontal resolution due to its high computational cost in the 6-hourly cycling experiments. All 6-hourly cycling experiments are conducted from March to July 2022 while the first month is excluded from evaluation as it is used as the assimilation spin-up (burn-in) period. To obtain LSM initial conditions at the beginning of the experiments (i.e., 1 March 2022), an offline spin-up of the Noah LSM is first run from 2008 to April 2020 forced by the meteorological forcing fields from the Global Land Data Assimilation System (GLDAS, Rodell et al., 2004), followed by additional spin-up until 1 March 2022 using the KIM atmospheric forcing, which is available only from May 2020 for the LSM offline simulation. The KIM atmospheric model is initialized by the fifth generation of the European Cen-

**Table 1.** Perturbation parameter values used for autoregressive temporal correlations and cross correlations between different variables (SW: shortwave radiation, LW: longwave radiation, P: precipitation, SM1: top layer soil moisture, SM2: second layer soil moisture, SM3: third layer soil moisture, and SM4: bottom layer soil moisture).

| Perturbed variables | Time scale of first-order autoregressive temporal correlations (hour) | Cross correlations with perturbations in | | | |
|---|---|---|---|---|---|
| KIM atmospheric forcing | | SW | LW | *P* | |
| SW | 24 | 1.0 | −0.5 | −0.8 | |
| LW | 24 | −0.5 | 1.0 | 0.5 | |
| *P* | 24 | −0.8 | 0.5 | 1.0 | |
| Noah LSM soil moisture | | SM1 | SM2 | SM3 | SM4 |
| SM1 | 12 | 1.0 | 0.6 | 0.4 | 0.2 |
| SM2 | 12 | 0.6 | 1.0 | 0.6 | 0.4 |
| SM3 | 12 | 0.4 | 0.6 | 1.0 | 0.6 |
| SM4 | 12 | 0.2 | 0.4 | 0.6 | 1.0 |

**Table 2.** Summary of land-atmosphere coupled data assimilation (DA) experiments conducted in this study (SM: soil moisture; see Appendix A for additional abbreviations).

| | CTL* | SG_AT | SG_SP* | MT_ATSP |
|---|---|---|---|---|
| Land | | | | |
| SM DA | X | O | O | O |
| SM data | – | ASCAT | SMAP | ASCAT + SMAP |
| SM bias correction method | – | CDF matching | anomaly correction | CDF matching (ASCAT); anomaly correction (SMAP) |
| SM DA scheme | – | EnKF | EnKF | EnKF |
| LSM | Noah LSM v2.7.1 (KIM-LSM) and v3.3 (LIS-LSM) | | | |
| LSM horizontal resolution | 25 km | | | |
| LSM ensemble size | 20 | | | |
| Atmosphere | | | | |
| KIM | KIM v3.9 | | | |
| KIM horizontal resolution | deterministic component (25 km); ensemble component (50 km) | | | |
| Atmospheric DA scheme | deterministic component (4DEnVar); ensemble component (LETKF) | | | |
| KIM ensemble size | 50 | | | |
| Experimental period | 1 April to 31 July 2022 (DA spin-up: 1 to 31 March 2022) | | | |

* Note that CTL and SG_SP are the same experiments as those presented in Kwon et al. (2024).

tre for Medium-Range Weather Forecasts (ECMWF) atmospheric reanalysis (ERA5, Hersbach et al., 2020). In addition to the cycling runs in each experimental case, 5 d forecasts are performed every 00:00 and 12:00 UTC cycle after being initialized by the land and atmospheric analyses from DA.

## 6 Performance evaluation

Due to the difficulty in acquiring a global ground truth reference dataset, we perform global-scale performance evaluations of the soil moisture DA for different hydrometeorological variables using datasets from various sources such as satellite-based observations and analysis fields from different systems. The four experiments (i.e., CTL, SG_AT, SG_SP, and MT_ATSP) listed in Table 2 are assessed in terms of generating the soil moisture analysis, specific humidity and air temperature analyses/forecasts, and precipitation forecasts. Methodologies and datasets employed in this study for the evaluation are described below.

### 6.1 Soil moisture

A triple collocation analysis (TCA, Stoffelen, 1998; Scipal et al., 2008), a statistical random error estimation method, is applied to evaluate the global soil moisture analysis from

the soil moisture DA experiments. TCA has been initially proposed by Stoffelen (1998) to quantify the error of near-surface ocean wind speed estimates, and it is now one of the most commonly used method for estimating uncertainties in satellite-based soil moisture retrievals (e.g., Dorigo et al., 2010; Gruber et al., 2016; Kim et al., 2021b, 2023; Scipal et al., 2008) or for evaluating large-scale soil moisture simulations of computational models (e.g., Kim et al., 2021a; Kwon et al., 2024; Nair and Indu, 2019; Renzullo et al., 2014) due to no requirement of reliable ground truth reference data that is hard to obtain at large scales.

The TCA approach is based on the assumption of a linear relationship between hypothetical true soil moisture and individual soil moisture estimates as expressed in Eq. (1):

$$\theta_k = \alpha_k + \beta_k \theta_{\text{true}} + \varepsilon_k \tag{1}$$

where $\theta_k$ is independent collocated soil moisture datasets (i.e., triplet components, $k \in [x, y, z]$); $\alpha_k$ and $\beta_k$ are additive and multiplicative systematic biases of $\theta_k$, respectively, with respect to the unknown hypothetical true soil moisture signal ($\theta_{\text{true}}$); and $\varepsilon_k$ represents the additive random noise in each soil moisture data ($\theta_k$). The random error (noise) variance ($\sigma^2_{\varepsilon_k}$) of three collocated soil moisture triplets [Eqs. (2) to (4)] can be derived from variance and covariance equations by introducing additional assumptions, i.e., error orthogonality (independence between the random error of the soil moisture datasets and the unknown soil moisture truth) and zero error-cross correlation (independence of the random errors between the soil moisture datasets) (Gruber et al., 2016).

$$\sigma^2_{\varepsilon_x} = \sigma^2_x - \frac{\sigma_{xy}\sigma_{xz}}{\sigma_{yz}} \tag{2}$$

$$\sigma^2_{\varepsilon_y} = \sigma^2_y - \frac{\sigma_{yx}\sigma_{yz}}{\sigma_{xz}} \tag{3}$$

$$\sigma^2_{\varepsilon_z} = \sigma^2_z - \frac{\sigma_{zx}\sigma_{zy}}{\sigma_{xy}} \tag{4}$$

where $\sigma^2_k$ and $\sigma^2_{\varepsilon_k}$ ($k \in [x, y, z]$) are the variance and random error variance, respectively, of each soil moisture data; and $\sigma_{xy}$, $\sigma_{xz}$, and $\sigma_{yz}$ are the covariances of two soil moisture triplet components. In this study, the fractional mean-square error ($\text{fMSE}_k$, Draper et al., 2013), ranging from 0 (free-of-noise soil moisture data) to 1 (no meaningful soil moisture signal), is computed using Eq. (5). This metric is employed as a TCA-based global soil moisture evaluation measure, following procedures implemented by Kim et al. (2020 and 2021a) and Kwon et al. (2024).

$$\text{fMSE}_k = \frac{\sigma^2_{\varepsilon_k}}{\sigma^2_k} \tag{5}$$

In order to meet the zero error-cross correlation assumption, we select two independent satellite-based soil moisture products, i.e., ASCAT and Advanced Microwave Scanning Radiometer 2 (AMSR2) [or Soil Moisture and Ocean Salinity (SMOS)], derived from different microwave sensors using different retrieval algorithms for the first and second soil moisture triplet components while the soil moisture simulations from the experiments (CTL, SG_AT, and SG_SP) are used for the third triplet component (Table 3). Due to the TCA assumptions, it is hard to compose the same reference frame for all experimental cases, especially for the multi-sensor soil moisture DA experiment. Therefore, for a fair comparison, we only evaluate the relative improvement in the soil moisture estimates by comparing fMSE of the single-sensor soil moisture DA with fMSE of CTL that are computed using the same first and second triplet components (i.e., satellite soil moisture retrievals that are not assimilated in the soil moisture DA experiment) as shown in Table 3. The effects of the multi-sensor soil moisture DA (MT_ATSP) are assessed only for atmospheric variables (see Sect. 6.2 and 6.3).

**Table 3.** Triple collocation analysis (TCA) triplet composition to quantify the relative improvement in the soil moisture estimates by soil moisture data assimilation (DA) as compared to CTL. The CTL soil moisture estimates are also evaluated using the same satellite-based reference soil moisture products as used for each single-sensor soil moisture DA experiment (EXP: SG_AT and SG_SP).

| Experiments | Triplets for EXP | Triplets for CTL |
|---|---|---|
| SG_AT | AMSR2, SMOS, SG_AT | AMSR2, SMOS, CTL |
| SG_SP | AMSR2, ASCAT, SG_SP | AMSR2, ASCAT, CTL |

The ASCAT, SMOS, and AMSR2 soil moisture data used in TCA are the 12.5 km ASCAT soil moisture Climate Data Record (CDR) version 7 product (H119 and extended H120) based on the TU-Wien change detection algorithm (Wagner et al., 2013), the SMOS-INRA-CESBIO (SMOS-IC) version 2 product, and the AMSR2 X-band Land Parameter Retrieval Model (LPRM) product, respectively. The original datasets are preprocessed by conducting quality control based on quality flags provided in each data product, and spatial resampling using the nearest neighbor distance method to match the spatial resolution of the datasets with that of the LSM outputs (i.e., 25 km latitude-longitude grids). Due to the different local overpass time between the satellite soil moisture products [i.e., 09:30 am/pm LST for ASCAT, 01:30 am/pm LST for ASMR2, and 06:00 am/pm LST for SMOS], the UTC-based Noah-LSM outputs at 04:00 am/pm LST and 11 am/pm LST are extracted for TCA that uses AMSR2/SMOS/SG_AT(or CTL) and AMSR2/ASCAT/SG_SP(or CTL), respectively. We select model outputs at the approximate midpoint time (e.g., 04:00) between the overpass times of two other satellite-based soil moisture triplet components (e.g., 01:30 AMSR2 and 06:00 SMOS) for a fair comparison. While some errors may still arise due to sampling-time mismatches between the triplet components, we assume these errors are acceptable since the same sampling time was applied to both CTL and DA experimental outputs to evaluate their relative per-

formance. Please refer to Kwon et al. (2024) and Kim et al. (2023) for more detailed procedures.

### 6.2 Specific humidity and air temperature

Evaluations of the specific humidity and air temperature analyses/forecasts are performed using the ECMWF Integrated Forecasting System (IFS) analysis (ECMWF, 2017) as reference data, which has been extensively used for evaluating modeling systems (e.g., Ben Bouallègue et al., 2024; Kwon et al., 2024; Lee et al., 2020; Polichtchouk et al., 2023; Reichle et al., 2023). The root mean square difference (RMSD) between the atmospheric variables (i.e., specific humidity and air temperature) from each experiment and those from the IFS analysis is computed.

### 6.3 Precipitation

Local variations in soil moisture modify boundary-layer heat and moisture fluxes, thereby altering water–energy budgets and influencing convective triggering (Findell and Eltahir, 2003; Pal and Eltahir, 2003) and subsequently influence large-scale dynamics (Cook et al., 2006; Pal and Eltahir, 2003), both of which play key roles in determining precipitation processes. A number of studies have investigated the complex interaction mechanisms between soil moisture and precipitation, referred to as the 'soil moisture-precipitation feedback', using observational analyses (e.g., Catalano et al., 2016; Yang et al., 2018) and computational modeling systems (e.g., Beljaars et al., 1996; Bosilovich and Sun, 1999; Hohenegger et al., 2009; Lin et al., 2023; Pal and Eltahir, 2003). Although these studies generally agree on a predominant positive feedback, the sign and strength vary depending on modeling systems and spatiotemporal scales (Hohenegger et al., 2009; Lin et al., 2023). Differences in the sign of soil moisture-precipitation feedback can be attributed to the complexity of representing the soil moisture-evapotranspiration relationship (Yang et al., 2018) and convective development (Hohenegger et al., 2009). Considerable debate and uncertainty remain regarding the physical mechanisms determining the sign of the feedback (Hohenegger et al., 2009). Nevertheless, there is no doubt that soil moisture and precipitation are reciprocally linked, implying that better characterization of soil moisture conditions through soil moisture DA can enhance precipitation forecasts in land-atmosphere coupled systems.

We assess the impact of soil moisture DA on precipitation forecast skill using well-established metrics, such as the frequency bias (FB) and equitable threat score (ETS) based on recommendations by the World Meteorological Organization (WMO, 2008). Calculations of the FB and ETS metrics are based on a $2 \times 2$ contingency table (Table 4), which consists of Hits, Misses, FalseAlarms, and CorrectNegatives. Gauge-based global daily precipitation analyses from the National Oceanic and Atmospheric Administration (NOAA) Climate Prediction Center (CPC) (Chen et al., 2008; Xie et al., 2007) are used as reference data for precipitation evaluation.

**Table 4.** Contingency table for computing precipitation forecast evaluation metrics.

| | | Observation (reference data) | |
|---|---|---|---|
| | | Yes | No |
| Forecast (model data) | Yes | Hits | FalseAlarms |
| | No | Misses | CorrectNegatives |

FB [Eq. (6)] assesses the ratio of the frequency of precipitation occurrence in the forecast to that in the observation:

$$\mathrm{FB} = \frac{\mathrm{Hits} + \mathrm{FalseAlarms}}{\mathrm{Hits} + \mathrm{Misses}} \tag{6}$$

where Hits, FalseAlarms, and Misses are the number of model grid points with correct forecasts, false alarms, and missed forecasts of precipitation occurrence, respectively. The FB metric ranges from zero to infinity where the ideal FB score is 1.0, indicating that the number of the forecasted precipitation events is the same as that of the observed events. Note that FB does not consider the timing of precipitation events.

ETS [Eq. (7)] quantifies the fraction of the forecasted or observed precipitation events that are captured correctly after excluding random hits ($\mathrm{Hits_{rnd}}$), which is the number of correct forecasts by random chance computed using Eq. (8):

$$\mathrm{ETS} = \frac{\mathrm{Hits} - \mathrm{Hits_{rnd}}}{\mathrm{Hits} + \mathrm{Misses} + \mathrm{FalseAlarms} - \mathrm{Hits_{rnd}}} \tag{7}$$

$$\mathrm{Hits_{rnd}} = \frac{(\mathrm{Hits} + \mathrm{Misses})(\mathrm{Hits} + \mathrm{FalseAlarms})}{N} \tag{8}$$

where $N$ is the total number of events defined as $N = \mathrm{Hits} + \mathrm{Misses} + \mathrm{FalseAlarms} + \mathrm{CorrectNegatives}$. CorrectNegatives denotes the number of correct forecasts of no precipitation. The ETS metric ranges from $-1/3$ to 1, where values below 0 and 1 represent "no skill" and "perfect skill" (no Misses or FalseAlarms), respectively.

## 7 Results

In this section, we first examine the performance of the KIM-LIS coupled system in producing enhanced global soil moisture estimates when the system is informed by satellite-based soil moisture retrievals from ASCAT and SMAP via assimilation. Next, the impacts of assimilating the ASCAT and SMAP soil moisture data, both individually and simultaneously, on atmospheric analyses and forecasts are assessed. Finally, we evaluate the added skill of the KIM-LIS system in forecasting precipitation when using initialized soil moisture conditions from multi-sensor soil moisture DA.

### 7.1 Soil moisture analysis

The impact of single-sensor soil moisture assimilation (i.e., SG_AT and SG_SP) on the global soil moisture estimates is evaluated using the TCA method (see Sect. 6.1). Figure 2 presents the spatial distribution of fMSE obtained from TCA during the experimental period from April to July 2022. Both ASCAT and SMAP are seen to have an overall positive impact on the surface soil moisture estimates of the Noah LSM through assimilation. Compared to the CTL experiment, which does not assimilate soil moisture data, SG_AT and SG_SP reduce the global mean fMSE by 4.0 % (Fig. 2a) and 10.5 % (Fig. 2b), respectively. In both single-sensor soil moisture DA cases, obvious improvements in soil moisture are observed in Asia while a decrease in skill is mostly found in the Australian and North American continents where CTL already exhibits a relatively good performance in estimating soil moisture.

Note that we use identical first and second triplet components for DA and CTL (Table 3), replacing only the CTL soil moisture estimates with those from the DA experiments (SG_AT and SG_SP) to assess the relative performance gain from soil moisture DA. This approach (i.e., replacing one triplet member) may alter the fMSE calculation of the other two triplet components and thus influence the comparison results between DA and CTL. However, because the soil moisture estimates from DA and CTL share the same spatial and temporal coverage and climatology, as they are generated from the identical modeling system, the impact of replacing the model-based triplet member is negligible, as shown in Fig. S1. Therefore, the fMSE comparison results (Fig. 2) can be considered reliable.

Because land surface characteristics affect the soil moisture skill of models and observations (Draper et al., 2012), the TCA results are also plotted for the MODIS-IGBP land cover types. Figure 3 shows that for all land cover types, both SG_AT and SG_SP enhance the skill of the modeled soil moisture relative to CTL in terms of the median fMSE, with SG_SP achieving greater skill gains. The soil moisture estimates are significantly improved by SG_AT for evergreen broadleaf forests and croplands, and by SG_SP for deciduous needleleaf forests, deciduous broadleaf forests, mixed forests, open shrublands, woody savannas, savannas, grasslands, croplands, and barren or sparsely vegetated land cover types. In both SG_AT and SG_SP experiments, the highest skill improvements, in terms of the median fMSE, are observed for croplands. This implies that the land DA system effectively utilizes soil moisture signals related to agricultural practices from satellite observations, especially in the case of SMAP soil moisture DA (SG_SP), which employs the anomaly-based bias correction approach.

Figures 2 and 3 indicate that SMAP DA shows higher skill than ASCAT DA for the soil moisture analysis. The superior performance of SMAP over ASCAT within a land DA system is also reported in Seo et al. (2021) where SMAP and ASCAT soil moisture DA results are evaluated against in situ measurements in the continental United States. These results can be supported by the fact that L-band brightness temperature measurements have higher sensitivity to soil moisture variations than C-band backscatter measurements (Kolassa et al., 2017), and thus the SMAP soil moisture retrievals have better accuracy (Al-Yaari et al., 2019; Kumar et al., 2018). However, note that in this study, a direct comparison of the global soil moisture analysis between SG_AT and SG_SP is not made because the model soil moisture outputs used in TCA are extracted at different LST – specifically, 04:00 am/pm for SG_AT and 11:00 am/pm for SG_SP – due to the different local overpass times of the satellite soil moisture data used for TCA-based assessment (see Sect. 6.1).

As shown in Fig. 2, soil moisture performance gains and losses by each single-sensor soil moisture DA are locally dependent. Thus, some previous studies (e.g., Draper et al., 2012; Kolassa et al., 2017) have shown that simultaneously assimilating soil moisture retrievals from both passive and active sensors achieves higher model soil moisture accuracy than assimilating a single product. However, because soil moisture triplets that fully satisfy the TCA assumptions (see Sect. 6.1) are difficult to obtain over the global domain for the multi-sensor soil moisture DA experiment, the combined effects of ASCAT and SMAP DA are discussed only in terms of atmospheric variables, which are the ultimate objective of this study, in the subsequent sections.

### 7.2 Analysis and forecast of specific humidity and air temperature

Domain-averaged RMSD differences (i.e., $RMSD_{EXP}$ minus $RMSD_{CTL}$) in the specific humidity analysis (Figs. 4a to 4c) and air temperature analysis (Fig. 4d to f) are evaluated across atmospheric levels and over time. Compared to CTL (without soil moisture DA), ASCAT DA (i.e., SG_AT) has more beneficial impacts on the air temperature analysis (Fig. 4d) while SMAP DA (i.e., SG_SP) has more beneficial impacts on the specific humidity analysis (Fig. 4b). Figure 4c and f show that the simultaneous assimilation of ASCAT and SMAP soil moisture retrievals (i.e., MT_ATSP) improves the analysis of both atmospheric variables relative to CTL. Notably, degradations in the specific humidity and air temperature analyses by SG_AT and SG_SP, respectively, are compensated by additionally assimilating other soil moisture products.

Figure 5 more clearly demonstrates that multi-sensor soil moisture DA enhances the performance of the specific humidity analyses (Fig. 5a) and air temperature analyses (Fig. 5d) compared to the single-sensor soil moisture DA cases (i.e., SG_AT and SG_SP, respectively). Although MT_ATSP exhibits somewhat reduced performance in the air temperature (Fig. 5c) and specific humidity analyses (Fig. 5b) compared to SG_AT and SG_SP, respectively, it achieves a more balanced improvement, meaning that neither

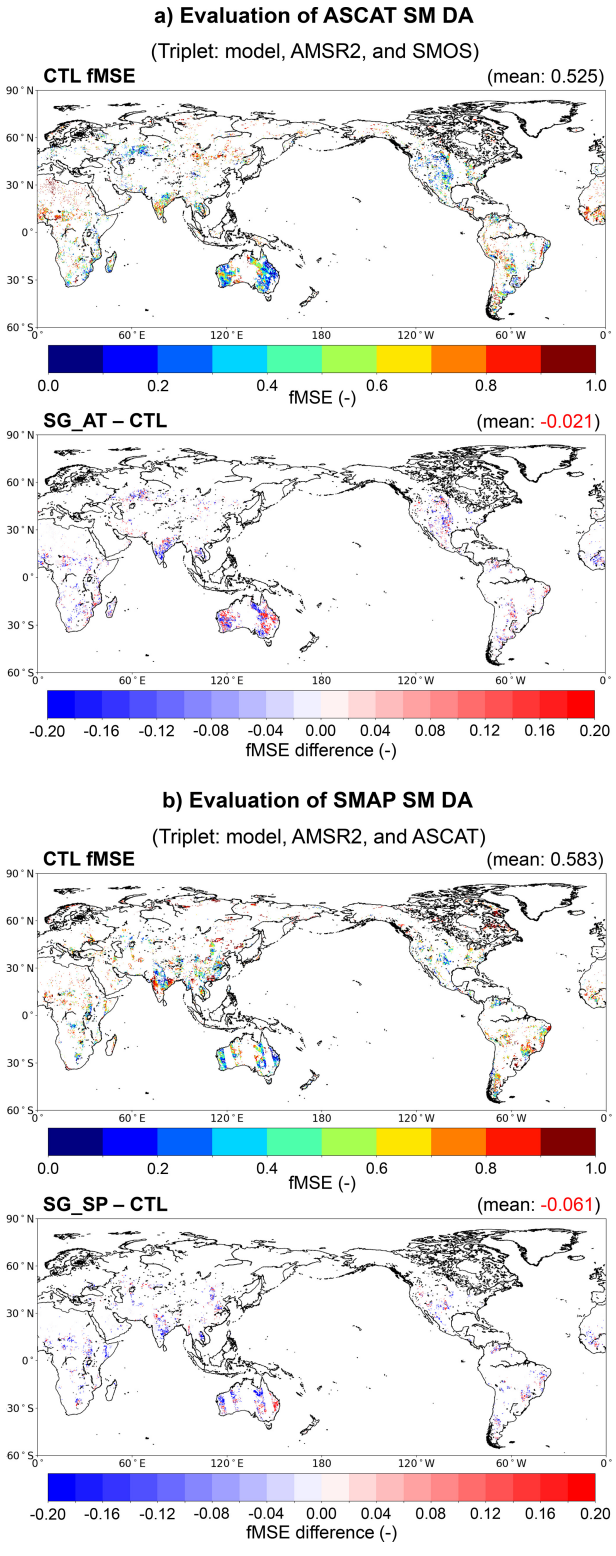


**Figure 2.** Global maps of the soil moisture triple collocation analysis (TCA) results for **(a)** ASCAT (i.e., SG_AT) and **(b)** SMAP soil moisture data assimilation (i.e., SG_SP). In each panel, the top subpanel shows the fractional mean-square error (fMSE) of CTL soil moisture at 04:00 am/pm local solar time (LST) in **(a)** and 11:00 am/pm LST in **(b)**. The bottom subpanel shows the soil moisture fMSE difference between SG_AT and CTL in **(a)** and between SG_SP and CTL in **(b)**. Negative fMSE differences indicate improved soil moisture estimates from ASCAT and SMAP data assimilation, respectively.

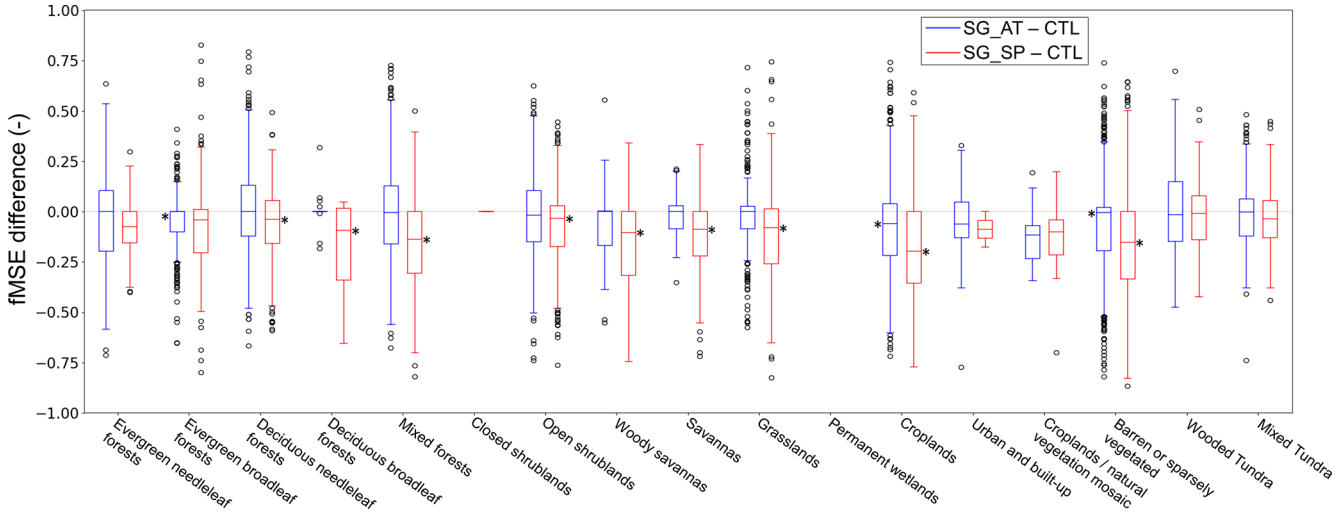


**Figure 3.** Differences in the soil moisture fractional mean-square error (fMSE) between the single-sensor soil moisture data assimilation (i.e., SG_AT and SG_SP) and control [without soil moisture data assimilation (DA); i.e., CTL] experiments depending on land cover types. A dominant land cover type in each model grid is obtained from the MODIS-IGBP land cover classifications (Friedl et al., 2002). The asterisk symbol (*) indicates statistical significance at $p<0.05$. Negative values represent the improved soil moisture estimates by soil moisture DA. Results are not plotted for closed shrublands and permanent wetlands because of missing triplet data.

variable is degraded while both show moderate gains compared to CTL, by assimilating radar- and radiometer-based soil moisture data together.

Tables 5 and 6 summarize the domain-averaged RMSD differences between the soil moisture DA experiments and CTL for the analyses and forecasts of 2 m atmospheric variables (i.e., specific humidity and air temperature) from the 00:00 UTC cycle (Table 5) and the 12:00 UTC cycle (Table 6). In the global domain, SG_SP generally achieves better domain-averaged analysis and forecast skills for both 2 m atmospheric variables compared to SG_AT (Tables 5 and 6), except for the 2 m air temperature forecast of the 12:00 UTC cycle, where SG_AT performs slightly better (Table 6). During the experimental period, all soil moisture DA cases are more effective in improving the 2 m air temperature analysis and forecast than those of specific humidity, especially for the 00:00 UTC cycle. Overall, they perform better in the Northern Hemisphere than in the Southern Hemisphere (Tables 5 and 6), although they achieve greater 2 m air temperature forecast skill during the 00:00 UTC cycle in the Southern Hemisphere (Table 5). The lower analysis and forecast skills of soil moisture DA in the Southern Hemisphere can be attributed to the use of spatially and temporally constant observations errors (see Sect. 4.2), which do not adequately reflect the relatively higher uncertainties in winter-period soil moisture data.

For the 2 m specific humidity estimates, the assimilation of SMAP soil moisture retrievals alone (SG_SP) achieves the best domain-averaged performance (Tables 5 and 6). MT_ATSP reduces RMSD compared to SG_AT by additionally assimilating the SMAP soil moisture data, but it exhibits relatively lower skill in specific humidity than SG_SP. However, in Europe and tropical regions, MT_ATSP provides improved 2 m specific humidity forecasts compared to SG_SP, particularly when both ASCAT and SMAP have a positive impact. The synergistic impacts of the combined assimilation of ASCAT and SMAP are evident in the 2 m air temperature analysis and forecast of the 00:00 UTC cycle (Table 5).

Local performance differences in the 2 m atmospheric analysis between the single-sensor soil moisture DA cases are clearly illustrated in Fig. 6, which is plotted for the 12:00 UTC cycle from June to July 2022. SG_AT and SG_SP exhibit opposite impacts on the atmospheric analysis, especially on specific humidity, over India, Eurasia, and Brazil. ASCAT DA (SG_AT) generally leads to the improved analyses of specific humidity and air temperature over India while SMAP DA (SG_SP) performs better in Eurasia (except for India and the southern part of West Asia) and Brazil. These discrepancies in the local performance of 2 m specific humidity between ASCAT and SMAP DA may contribute to the reduced domain-averaged skill of MT_ATSP relative to SG_SP, as shown in Tables 5 and 6. In Africa, SG_AT yields better air temperature analysis than SG_SP, whereas SG_SP outperforms SG_AT in the specific humidity analysis. It can be noted from Fig. 6 that, locally, the joint assimilation of the ASCAT and SMAP soil moisture retrievals yields the best estimates of the 2 m atmospheric variables when both soil moisture products have positive impacts.

### 7.3 Precipitation

The potential added value of multi-sensor soil moisture DA for precipitation forecasts is assessed using categori-

https://doi.org/10.5194/hess-30-1261-2026

**Table 5.** Domain-averaged RMSD differences ($\Delta\text{RMSD} = \text{RMSD}_{\text{EXP}} - \text{RMSD}_{\text{CTL}}$) for the 2 m specific humidity and air temperature analyses and (5 d) forecasts across six domains [i.e., global domain (GLOB), Northern Hemisphere (NH), Southern Hemisphere (SH), Asia (ASIA), Europe (EU), and tropical area (TROP)]. The RMSD is calculated for the 00:00 UTC cycle from April to July 2022 (whole experimental period) using the ECMWF-IFS analysis as reference data. Negative ΔRMSD (bold) indicates improved estimates of the atmospheric variables by assimilating the soil moisture retrievals.

| April to July 2022 (00:00 UTC) | 2 m specific humidity ΔRMSD (EXP − CTL) [g kg$^{-1}$] | | | | | | | | | | | | | | | | | |
|---|---|---|---|---|---|---|---|---|---|---|---|---|---|---|---|---|---|---|
| | Analysis | | | Forecast | | | | | | | | | | | | | | |
| | | | | 1 d lead time | | | 2 d lead time | | | 3 d lead time | | | 4 d lead time | | | 5 d lead time | | |
| Domain | SG_AT | SG_SP | MT_ATSP | SG_AT | SG_SP | MT_ATSP | SG_AT | SG_SP | MT_ATSP | SG_AT | SG_SP | MT_ATSP | SG_AT | SG_SP | MT_ATSP | SG_AT | SG_SP | MT_ATSP |
| GLOB | 0.011 | **−0.001** | 0.001 | 0.012 | 0.001 | 0.002 | 0.014 | 0.004 | 0.005 | 0.013 | 0.004 | 0.004 | 0.014 | 0.004 | 0.006 | 0.017 | 0.004 | 0.010 |
| NH | 0.005 | **−0.006** | **−0.005** | 0.005 | **−0.004** | **−0.004** | 0.006 | **−0.002** | **−0.001** | 0.006 | **−0.002** | **−0.001** | 0.005 | **−0.004** | 0.000 | 0.009 | **−0.005** | 0.001 |
| SH | 0.046 | 0.025 | 0.040 | 0.029 | 0.011 | 0.016 | 0.026 | 0.010 | 0.012 | 0.017 | 0.006 | 0.007 | 0.018 | 0.007 | 0.009 | 0.022 | 0.016 | 0.025 |
| ASIA | 0.004 | **−0.004** | **−0.002** | 0.003 | **−0.001** | 0.000 | 0.006 | 0.002 | 0.003 | 0.008 | 0.004 | 0.004 | 0.009 | 0.003 | 0.006 | 0.009 | 0.006 | 0.010 |
| EU | 0.016 | **−0.001** | 0.003 | 0.012 | **−0.002** | **−0.004** | 0.010 | **−0.000** | **−0.005** | 0.004 | **−0.001** | **−0.006** | 0.002 | 0.006 | 0.000 | 0.002 | 0.003 | 0.001 |
| TROP | 0.008 | **−0.001** | **−0.004** | 0.016 | 0.005 | 0.005 | 0.021 | 0.011 | 0.010 | 0.022 | 0.012 | 0.011 | 0.023 | 0.013 | 0.013 | 0.025 | 0.014 | 0.017 |
| | 2 m air temperature ΔRMSD (EXP − CTL) [K] | | | | | | | | | | | | | | | | | |
| | Analysis | | | Forecast | | | | | | | | | | | | | | |
| | | | | 1 d lead time | | | 2 d lead time | | | 3 d lead time | | | 4 d lead time | | | 5 d lead time | | |
| Domain | SG_AT | SG_SP | MT_ATSP | SG_AT | SG_SP | MT_ATSP | SG_AT | SG_SP | MT_ATSP | SG_AT | SG_SP | MT_ATSP | SG_AT | SG_SP | MT_ATSP | SG_AT | SG_SP | MT_ATSP |
| GLOB | 0.001 | 0.000 | **−0.003** | **−0.000** | **−0.014** | **−0.013** | 0.001 | **−0.013** | **−0.011** | 0.001 | **−0.011** | **−0.010** | 0.003 | **−0.010** | **−0.008** | 0.005 | **−0.009** | **−0.003** |
| NH | 0.001 | **−0.008** | **−0.007** | 0.002 | **−0.005** | **−0.005** | 0.007 | 0.002 | 0.002 | 0.010 | 0.006 | 0.006 | 0.013 | 0.009 | 0.011 | 0.015 | 0.008 | 0.017 |
| SH | 0.016 | 0.002 | **−0.003** | 0.006 | **−0.012** | **−0.009** | **−0.006** | **−0.027** | **−0.022** | **−0.016** | **−0.028** | **−0.028** | **−0.019** | **−0.033** | **−0.029** | **−0.012** | **−0.021** | **−0.024** |
| ASIA | **−0.000** | **−0.007** | **−0.003** | **−0.001** | **−0.009** | **−0.025** | **−0.003** | **−0.009** | **−0.029** | **−0.003** | **−0.007** | **−0.029** | 0.002 | **−0.003** | **−0.020** | 0.005 | **−0.009** | **−0.015** |
| EU | **−0.005** | **−0.011** | **−0.010** | **−0.009** | **−0.033** | **−0.027** | **−0.001** | **−0.027** | **−0.019** | **−0.000** | **−0.026** | **−0.019** | **−0.003** | **−0.026** | **−0.019** | **−0.012** | **−0.038** | **−0.022** |
| TROP | **−0.005** | 0.012 | 0.001 | **−0.005** | **−0.027** | **−0.027** | **−0.006** | **−0.030** | **−0.028** | **−0.008** | **−0.032** | **−0.029** | **−0.007** | **−0.030** | **−0.029** | **−0.005** | **−0.030** | **−0.027** |

**Table 6.** Same as Table 5 but for the 12:00 UTC cycle from April to July 2022 (whole experimental period).

| April to July 2022 (12:00 UTC) | 2 m specific humidity ΔRMSD (EXP − CTL) [g kg$^{-1}$] | | | | | | | | | | | | | | | | | |
|---|---|---|---|---|---|---|---|---|---|---|---|---|---|---|---|---|---|---|
| | Analysis | | | Forecast | | | | | | | | | | | | | | |
| | | | | 1 d lead time | | | 2 d lead time | | | 3 d lead time | | | 4 d lead time | | | 5 d lead time | | |
| Domain | SG_AT | SG_SP | MT_ATSP | SG_AT | SG_SP | MT_ATSP | SG_AT | SG_SP | MT_ATSP | SG_AT | SG_SP | MT_ATSP | SG_AT | SG_SP | MT_ATSP | SG_AT | SG_SP | MT_ATSP |
| GLOB | 0.014 | 0.004 | 0.006 | 0.015 | 0.008 | 0.010 | 0.019 | 0.010 | 0.014 | 0.018 | 0.011 | 0.015 | 0.017 | 0.011 | 0.016 | 0.019 | 0.012 | 0.019 |
| NH | 0.003 | **−0.006** | **−0.005** | 0.005 | **−0.009** | **−0.006** | 0.007 | **−0.007** | **−0.001** | 0.006 | **−0.004** | 0.002 | 0.005 | **−0.004** | 0.002 | 0.008 | **−0.006** | 0.003 |
| SH | 0.052 | 0.026 | 0.036 | 0.064 | 0.040 | 0.050 | 0.060 | 0.033 | 0.045 | 0.053 | 0.029 | 0.041 | 0.046 | 0.027 | 0.042 | 0.046 | 0.030 | 0.046 |
| ASIA | 0.006 | 0.002 | 0.003 | 0.007 | **−0.002** | 0.001 | 0.011 | **−0.000** | 0.007 | 0.009 | 0.004 | 0.014 | 0.009 | 0.005 | 0.014 | 0.011 | 0.000 | 0.016 |
| EU | **−0.003** | **−0.007** | **−0.009** | **−0.003** | **−0.005** | **−0.009** | **−0.004** | 0.000 | **−0.007** | **−0.008** | 0.000 | **−0.008** | **−0.011** | 0.005 | **−0.005** | **−0.014** | 0.003 | 0.003 |
| TROP | 0.018 | 0.013 | 0.013 | 0.013 | 0.022 | 0.019 | 0.021 | 0.026 | 0.026 | 0.023 | 0.027 | 0.026 | 0.027 | 0.028 | 0.029 | 0.026 | 0.030 | 0.033 |

| | 2 m air temperature ΔRMSD (EXP − CTL) [K] | | | | | | | | | | | | | | | | | |
|---|---|---|---|---|---|---|---|---|---|---|---|---|---|---|---|---|---|---|
| | Analysis | | | Forecast | | | | | | | | | | | | | | |
| | | | | 1 d lead time | | | 2 d lead time | | | 3 d lead time | | | 4 d lead time | | | 5 d lead time | | |
| Domain | SG_AT | SG_SP | MT_ATSP | SG_AT | SG_SP | MT_ATSP | SG_AT | SG_SP | MT_ATSP | SG_AT | SG_SP | MT_ATSP | SG_AT | SG_SP | MT_ATSP | SG_AT | SG_SP | MT_ATSP |
| GLOB | **−0.007** | **−0.010** | **−0.015** | 0.005 | 0.018 | 0.012 | 0.008 | 0.018 | 0.012 | 0.009 | 0.019 | 0.015 | 0.007 | 0.017 | 0.011 | 0.008 | 0.018 | 0.011 |
| NH | 0.002 | **−0.004** | **−0.007** | **−0.002** | **−0.008** | **−0.008** | **−0.000** | **−0.012** | **−0.009** | **−0.003** | **−0.015** | **−0.011** | **−0.004** | **−0.018** | **−0.018** | **−0.002** | **−0.018** | **−0.017** |
| SH | 0.008 | **−0.001** | **−0.004** | 0.070 | 0.037 | 0.051 | 0.082 | 0.045 | 0.060 | 0.087 | 0.050 | 0.071 | 0.091 | 0.060 | 0.079 | 0.082 | 0.056 | 0.073 |
| ASIA | **−0.006** | **−0.010** | **−0.018** | 0.002 | **−0.004** | **−0.002** | 0.011 | **−0.003** | 0.004 | 0.010 | **−0.007** | 0.004 | 0.009 | **−0.016** | **−0.006** | 0.015 | **−0.017** | 0.001 |
| EU | 0.000 | **−0.003** | **−0.000** | **−0.021** | **−0.004** | **−0.008** | **−0.026** | **−0.001** | **−0.011** | **−0.031** | 0.003 | **−0.015** | **−0.032** | 0.008 | **−0.020** | **−0.033** | 0.018 | **−0.009** |
| TROP | **−0.024** | **−0.021** | **−0.029** | **−0.007** | 0.049 | 0.026 | **−0.003** | 0.053 | 0.027 | **−0.000** | 0.058 | 0.033 | **−0.003** | 0.054 | 0.031 | **−0.000** | 0.058 | 0.031 |

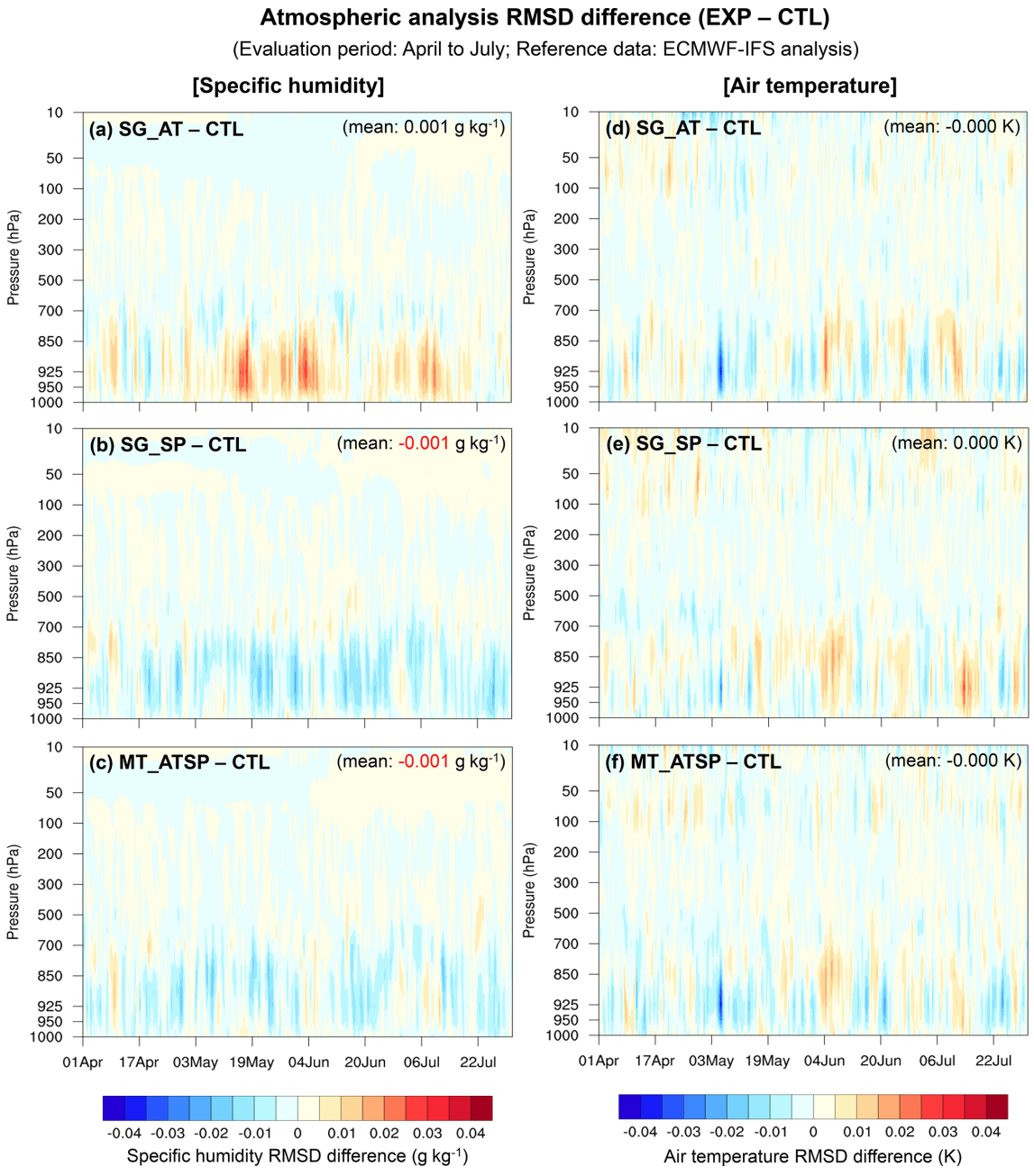


**Figure 4.** Vertical profile time series of RMSD differences in the specific humidity analysis (left column) and air temperature analysis (right column) between the soil moisture data assimilation (DA) and CTL experiments. The RMSD is calculated using the ECMWF-IFS analysis as reference data. Negative RMSD differences indicate improved estimates of the atmospheric variables by assimilating the soil moisture retrievals.

cal skill score metrics, including the FB and ETS, as detailed in Sect. 6.3. Daily precipitation rates (mm $d^{-1}$) are computed from the KIM forecasts at 0–24, 24–48, and 48–72 h lead times, and compared against reference data using seven conventional thresholds (0.5, 1.0, 5.0, 10.0, 15.0, 20.0, and 25.0 mm $d^{-1}$). The numbers of model grid points classified as Hits, FalseAlarms, Misses, and CorrectNegatives in the contingency table (Table 4) are then counted, and FB and ETS are calculated for six domains (i.e., global domain, Northern Hemisphere, Southern Hemisphere, Asia, Europe, and tropical area). Figure S2 presents the FB and ETS of daily precipitation forecasts from KIM, averaged over the three lead times, for CTL and the three soil moisture DA experiments (SG_AT, SG_SP, and MT_ATSP) during the 00:00 UTC cycle in July 2022. The corresponding

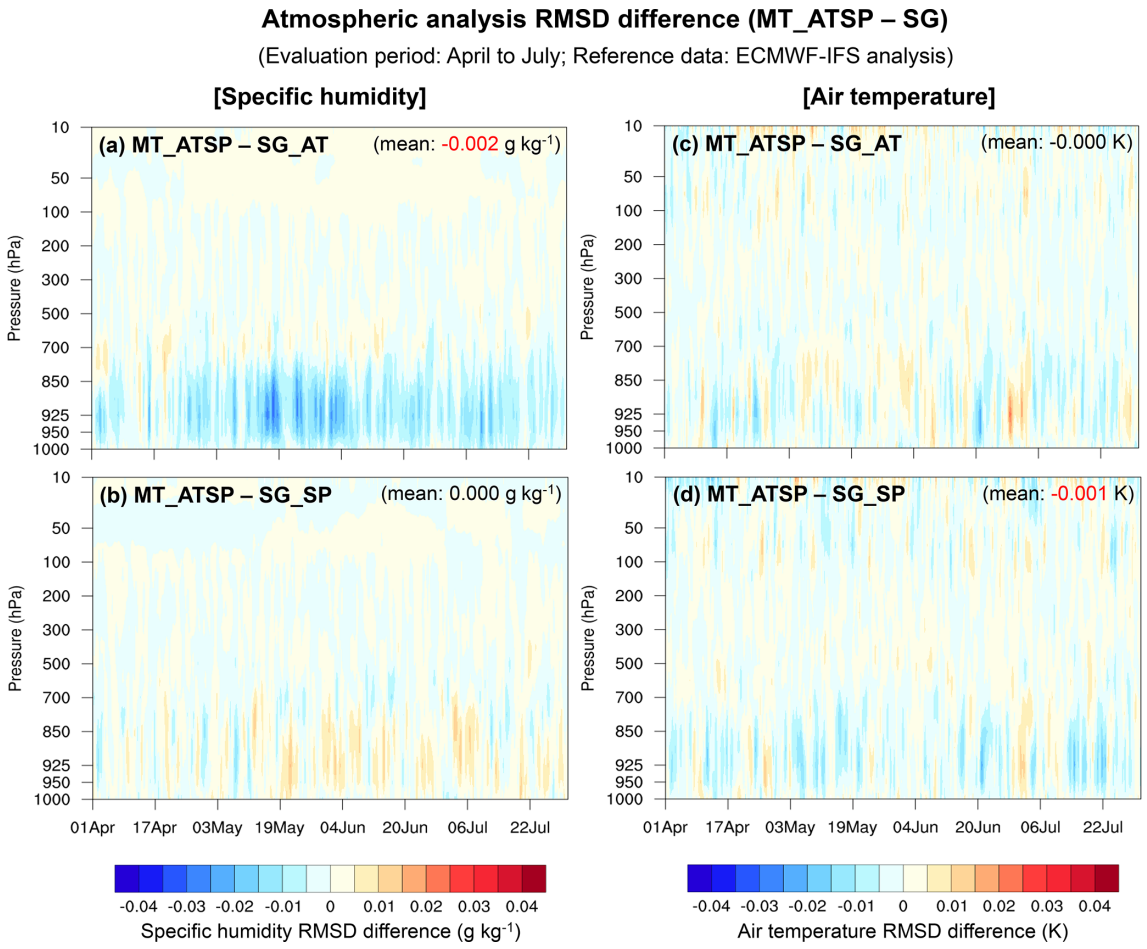


**Figure 5.** Vertical profile time series of RMSD differences in the specific humidity analysis (left column) and air temperature analysis (right column) between the multi-sensor soil moisture data assimilation (DA) (MT_ATSP) and single-sensor soil moisture DA [SG_AT (**a** and **c**) and SG_SP (**b** and **d**)] experiments. The RMSD is calculated using the ECMWF-IFS analysis as reference data. Negative RMSD differences indicate improved estimates of the atmospheric variables by additionally assimilating the SMAP or ASCAT soil moisture retrievals.

differences ($\Delta FB = |FB_{EXP} - 1| - |FB_{CTL} - 1|$, $\Delta ETS = ETS_{EXP} - ETS_{CTL}$) are shown in Fig. 7.

In the global domain, CTL (without soil moisture DA) tends to overestimate precipitation frequency (FB > 1.0), simulating excessive precipitation events, except for the precipitation threshold of 25.0 mm d$^{-1}$ (Fig. S2a). The model significantly overestimates precipitation at the 5.0 mm d$^{-1}$ threshold and exhibits an FB close to 1 for heavier precipitation events (20.0 and 25.0 mm d$^{-1}$) (Fig. S2a), with regional variations (Fig. S2b to f). Both the smallest FB (close to 1.0) and the largest FB (>2.5) are observed in the Southern Hemisphere for the lightest (0.5 mm d$^{-1}$) and heaviest (25.0 mm d$^{-1}$) precipitation events, respectively (Fig. S2c).

Unlike FB, ETS is higher (indicating better skill in predicting precipitation events) at lower precipitation thresholds while ETS decreases as the precipitation intensity thresholds increase in the global domain (Fig. S2g) and in the Northern Hemisphere (Fig. S2h), including Asia (Fig. S2j), Europe (Fig. S2k), and tropical areas (Fig. S2l). In the Southern Hemisphere, CTL shows the highest ETS skill at the precipitation threshold of 10.0 mm d$^{-1}$ and the lowest at 1.0 mm d$^{-1}$ (Fig. S2i). The different model performance patterns (in both FB and ETS) between the Northern and Southern Hemispheres across the range of precipitation intensity thresholds may be attributed to different weather regimes associated with cyclones and monsoons (Dare and Ebert, 2017), along with additional impacts from seasonal variations.

Overall, soil moisture DA improves the prediction of precipitation events (i.e., better ETS; Fig. 7g) while its contribution to precipitation frequency (FB) remains neutral (Fig. 7a). MT_ATSP demonstrates higher ETS skill than CTL (by up to 1.8 %) and single-sensor soil moisture DA (by up to 2.4 % and 0.6 % relative to SG_AT and SG_SP, respectively) (Fig. 7g). The impacts of MT_ATSP on the global FB are marginal, showing negligible improvements at the 0.5, 1.0, 5.0, and 25.0 mm d$^{-1}$ thresholds and slight overpredictions at the 10.0, 15.0, and 20.0 mm d$^{-1}$ thresholds (Figs. 7a, S2a). Similar soil moisture DA performance

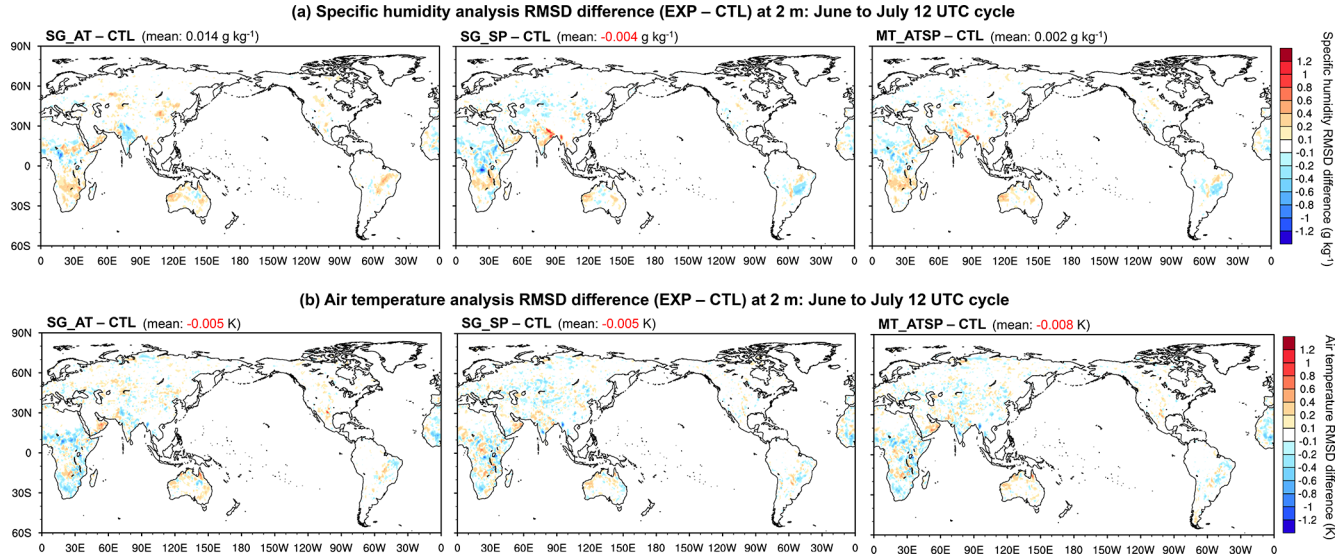


**Figure 6.** Differences in the 2 m atmospheric analysis RMSD [i.e., specific humidity (upper panels) and air temperature (lower panels)] between the soil moisture data assimilation (DA) and CTL experiments. Evaluation results for the 12:00 UTC cycle from June to July 2022 (a two-month period) are presented with domain-averaged values in parenthesis. The RMSD is calculated using the ECMWF-IFS analysis as reference data. Negative RMSD differences indicate improved estimates of the atmospheric variables by assimilating the soil moisture retrievals.

patterns are observed in the Northern Hemisphere (Fig. 7b and h) and Asia (Fig. 7d and j). In the Southern Hemisphere, MT_ATSP slightly improves FB for heavy precipitation events (precipitation thresholds $\geq 15.0\,\mathrm{mm\,d^{-1}}$) while relatively obvious improvements in ETS by MT_ATSP are witnessed at lower thresholds ($\leq 1.0\,\mathrm{mm\,d^{-1}}$) (Fig. 7c and i). Compared to CTL and SG_AT, multi-sensor soil moisture DA enhances ETS across precipitation thresholds in tropical areas, although it is slightly less effective than SG_SP at thresholds $\leq 5.0\,\mathrm{mm\,d^{-1}}$ (Fig. 7l). For FB, MT_ATSP shows improvements over CTL and SG_AT in tropical areas, except at thresholds of 5.0 and $10.0\,\mathrm{mm\,d^{-1}}$, where SG_SP performs better (Fig. 7f). In contrast, MT_ATSP is generally ineffective in Europe (Fig. 7e and k), except for ETS at precipitation thresholds of $5.0\,\mathrm{mm\,d^{-1}}$ or lower. The overprediction of precipitation in Europe (Figs. 7e, S2e), especially for heavy precipitation events ($\geq 15.0\,\mathrm{mm\,d^{-1}}$), may lead to a decrease in ETS (Figs. 7k, S2k).

The regional variability in precipitation performance between the CTL and soil moisture DA experiments may be attributed to seasonality. A full-year or multi-year experiment would therefore be valuable in future studies to assess the impact of seasonality on the effectiveness of multi-sensor soil moisture DA for improving precipitation forecasts.

## 8 Discussion

### 8.1 ASCAT data assimilation

The experimental results indicate that SMAP DA slightly outperforms ASCAT DA in enhancing near-surface atmospheric analyses and forecasts. While many factors may affect the overall performance of each experiment, one factor may be related to errors resulting from subsurface scattering, which are not accounted for in the ASCAT soil moisture data used in this study, as discussed by Wagner et al. (2024). The current TU Wien change detection algorithm (Wagner et al., 1999, 2010), used to retrieve soil moisture from ASCAT backscatter observations, is based on the assumption of a positive linear relationship between soil backscatter and wetness. However, Wagner et al. (2024) demonstrated that this assumption fails when coarse fragments (e.g., stones and rocks) or discontinuities exist in the soil profile, as they increase subsurface scattering contributions to total backscatter signals under dry soil conditions. This eventually reverses the relationship between backscatter signals and soil moisture content, deteriorating the quality of soil moisture data retrieved with the current algorithm in many arid and semi-arid regions. This phenomenon partly explains why ASCAT DA exhibits better performance in croplands than in barren or sparsely vegetated areas, as shown in Fig. 3, which is consistent with results from soil moisture data evaluation studies (e.g., Dorigo et al., 2010).

Soil moisture bias correction methods used to remove systematic discrepancies between observations and models may

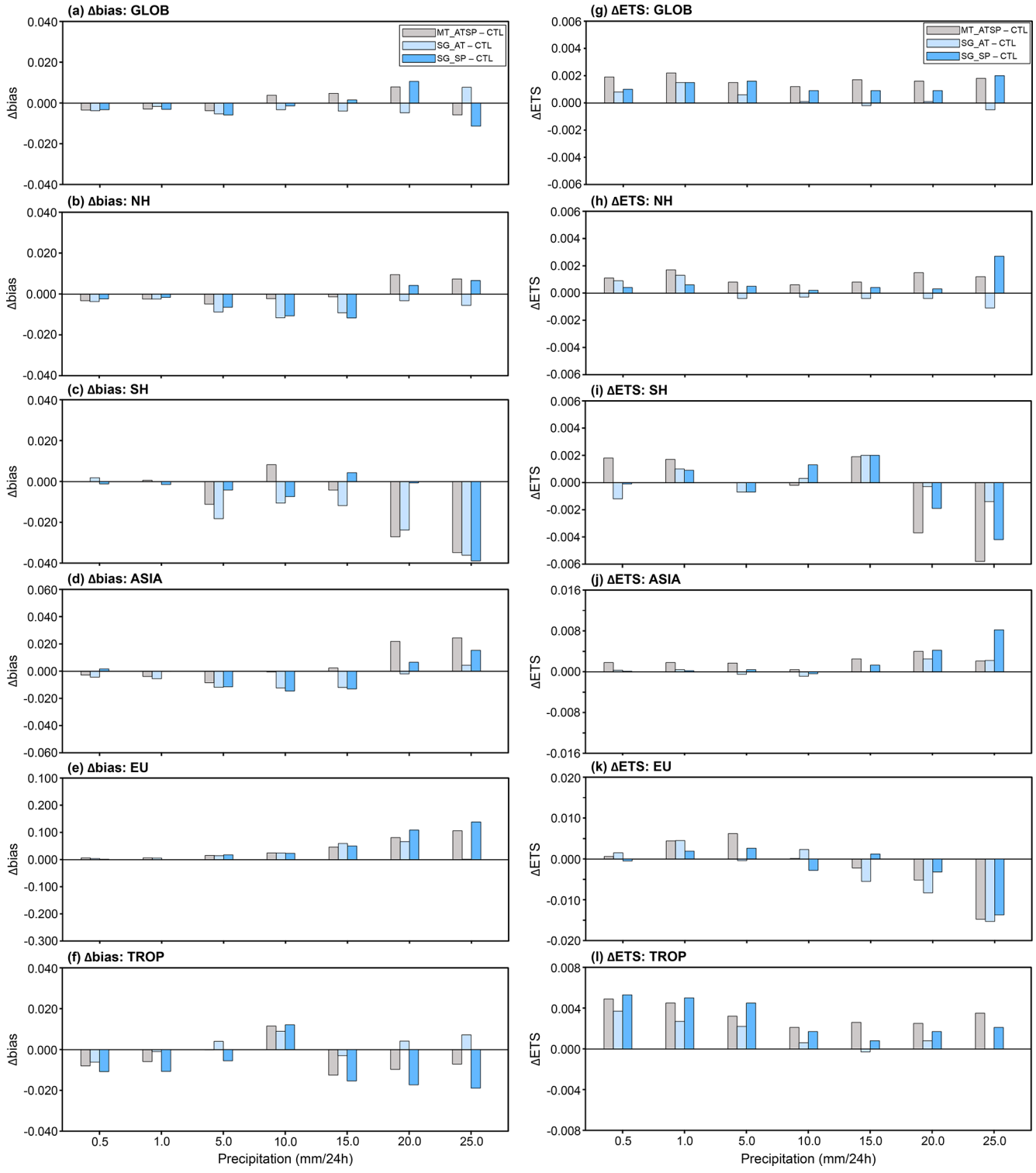


**Figure 7.** Differences in frequency bias ($\Delta FB = |FB_{EXP} - 1| - |FB_{CTL} - 1|$; **a** to **f**) and equitable threat score ($\Delta ETS = ETS_{EXP} - ETS_{CTL}$; **g** to **l**) between EXP (MT_ATSP, SG_AT, and SG_SP) and CTL, averaged over 24–72 h precipitation forecasts from the 00:00 UTC cycle in July 2022, for six domains [i.e., global domain (GLOB; **a** and **g**), Northern Hemisphere (NH; **b** and **h**), Southern Hemisphere (SH; **c** and **i**), Asia (ASIA; **d** and **j**), Europe (EU; **e** and **k**), and tropical area (TROP; **f** and **l**)]. The skill metrics are computed for seven conventional thresholds (i.e., 0.5, 1.0, 5.0, 10.0, 15.0, 20.0, and 25.0 mm $d^{-1}$). Negative ΔFB and positive ΔETS values indicate improvements from soil moisture DA.

also influence the ASCAT soil moisture DA performance. Kumar et al. (2015) and Kwon et al. (2022, 2024) have shown that different bias correction methods can substantially impact soil moisture DA performance. In SMAP DA, soil moisture temporal variability information is directly assimilated (i.e., anomaly correction method). In contrast, ASCAT DA employs the CDF matching method because it does not satisfy the underlying assumption of the anomaly correction method (see Sect. 3.3). It is a known issue that rescaling-based bias correction, such as CDF matching, causes a significant loss of information (Kumar et al., 2015). Meanwhile, Sect. S2 of the Supplementary Material and Figs. S3–S5 suggest that employing the anomaly correction method in soil moisture DA worsens the atmospheric analysis within land-atmosphere coupled systems when the underlying assumptions of the anomaly correction approach are not met. Rather than relying on CDF matching and anomaly correction methods, a more robust and appropriate bias correction approach is required for improving ASCAT soil moisture DA.

### 8.2 Soil moisture observation error

The effectiveness of the combined assimilation of multiple soil moisture products from different sources (i.e., radar backscatter and radiometer brightness temperature observations) in enhancing the soil moisture analysis skill has been demonstrated in previous studies (e.g., Blyverket et al., 2019; Draper et al., 2012; Kolassa et al., 2017; Renzullo et al., 2014). Our experimental results also show that, compared to single-sensor soil moisture DA, simultaneous assimilation of the ASCAT and SMAP soil moisture retrievals within the KIM-LIS coupled system has a synergistic impact, improving the analyses and forecasts of atmospheric variables including specific humidity, air temperature, and precipitation. However, the superiority of individual single-sensor soil moisture retrieval products and their combined performance within the DA system depend on the region and time period (Fig. 6). Specifically, locally reduced benefits of SMAP or ASCAT are observed in the multi-sensor soil moisture DA experiment when their performance impacts are opposite (Fig. 6). This may be attributed to the use of uniform observation error standard deviations for the soil moisture retrievals across space and time, which is unrealistic and does not adequately reflect the actual and relative retrieval skill of each soil moisture product. Especially, underestimated soil moisture observation errors can degrade the soil moisture and atmospheric analyses by over-relying on less reliable soil moisture data within the DA framework.

One key advantage of simultaneously assimilating individual soil moisture products, rather than a preprocessed multi-sensor-derived soil moisture product, is the flexibility to handle individual soil moisture sensors separately within a single DA system while achieving comparable performance (Kolassa et al., 2017). However, this advantage can be more effectively utilized by accurately specifying the relative errors of the soil moisture retrievals in space and time, enabling the optimal combination of models and diverse soil moisture products.

Several recent studies (e.g., Wu et al., 2021; Kim et al., 2023; Kim et al., 2025) have made efforts to estimate spatially or spatiotemporally distributed errors in satellite-based soil moisture retrievals using TCA-based methods and machine learning algorithms. A map of spatially distributed (but time-invariant) error standard deviations from Kim et al. (2025) [see Fig. S6, which is Fig. 5a in Kim et al. (2025)] exhibits that the SMAP soil moisture data have errors greater than $0.05\,m^3\,m^{-3}$ in many areas, particularly in forests. Excluding forested areas where soil moisture retrievals are masked out during quality control (see Sect. 3.4) and thus not assimilated, the error standard deviations of SMAP soil moisture are still above $0.02\,m^3\,m^{-3}$ (the uniformly applied error value in this study) in some savanna regions of South America and Africa, grasslands in North America, and croplands in South Asia (Fig. S6) [see Fig. S3c for the land-cover type map generated in this study using the MODIS-IGBP global land-cover classification (Friedl et al., 2002)]. As a result, this leads to degradation in the 2 m specific humidity and air temperature analyses in the regions, as noted in the SMAP soil moisture DA (SG_SP) results shown in Fig. 6.

Meanwhile, in ASCAT soil moisture DA, the spatially distributed soil moisture observation error standard deviation ($m^3\,m^{-3}$) (Fig. 8) is applied after locally rescaling the uniformly specified 10 % soil wetness index observation error using the ratio of the standard deviations of modeled and observed soil moisture time series (see Sect. 4.2). However, the spatial pattern of the ASCAT observation error standard deviations in Fig. 8 does not completely match that of the TCA/ML-based ASCAT fMSE computed by Kim et al. (2023) (see their Fig. 4f), which was derived using other satellite soil moisture data as triplet components. Notably, the ASCAT errors used in the current study appear to be relatively underestimated in dry areas of Africa and Asia (Fig. 8), where the 2 m atmospheric analyses are degraded by ASCAT soil moisture DA (SG_AT in Fig. 6).

The use of pre-generated spatial or spatiotemporal observation error estimates (e.g., Kim et al., 2025) can potentially maximize the benefits of each soil moisture product in multi-sensor soil moisture DA systems. One critical issue, however, is that bias correction of soil moisture observations, an essential procedure in soil moisture DA, may substantially alter their error characteristics, especially when rescaling-based methods like CDF matching are employed. To effectively apply spatially and temporally varying observation error estimates in multi-sensor soil moisture DA, a refined approach is needed to propagate error estimates from original soil moisture retrievals to bias-corrected soil moisture values.

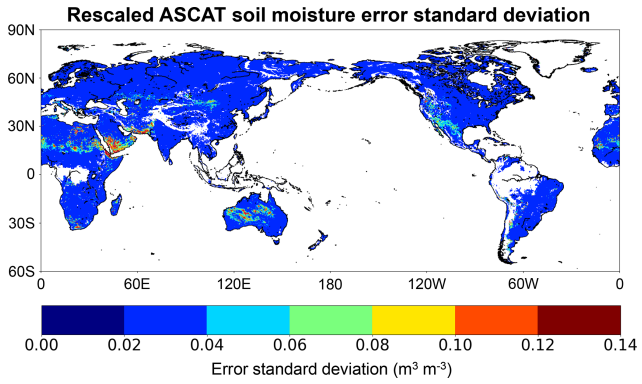


**Figure 8.** ASCAT soil moisture error standard deviations used for ASCAT soil moisture data assimilation (DA) in this study. The spatially distributed ASCAT soil moisture errors ($m^3\ m^{-3}$) are derived by rescaling the constant 10 % soil wetness index using the ratio of the standard deviations of the Noah land surface model (LSM) and ASCAT soil moisture time series.

## 9 Conclusions

This study develops and evaluates the NASA LIS-based multi-sensor soil moisture DA framework as part of the Korean Integrated Model (KIM) weather prediction system. The primary objective is to investigate the impact of simultaneously assimilating satellite-based near-surface soil moisture retrievals from C-band active radar (ASCAT) and L-band passive radiometer (SMAP) observations on the weather prediction performance of the KIM-LIS-based land-atmosphere weakly coupled DA system. The ASCAT and SMAP soil moisture data are assimilated individually (single-sensor DA) and jointly (multi-sensor DA) into the Noah LSM within the KIM-LIS system, and their relative and combined efficiencies in improving the global soil moisture analysis and atmospheric analysis/forecast skills are evaluated. Soil moisture DA is conducted using the 1-dimensional EnKF, while atmospheric DA is implemented using the hybrid 4DEnVar method with 4DIAU. The experiments are performed in the global domain based on 6 h cycling runs, which include analysis and forecast, followed by 5 d predictions at 00:00 and 12:00 UTC cycles.

TCA-based evaluations indicate that assimilating either ASCAT or SMAP soil moisture data results in an overall positive effect on the global soil moisture analysis performance of the Noah LSM, with global mean performance improvements of 4.0 % and 10.5 %, respectively. Both single-sensor soil moisture DA cases (i.e., ASCAT and SMAP) enhance the soil moisture performance across land cover types, with the greatest performance gains observed in croplands. It should be noted that although this study employs the TCA method as an alternative global-scale soil moisture evaluation approach, it has limitations, particularly in constructing TCA triplets for the multi-sensor soil moisture DA experiment without violating underlying assumptions. Therefore, we applied TCA only to the single-sensor DA experiments, and the overall benefit of assimilating both sensors simultaneously can only be inferred from the single-sensor results and the atmospheric evaluation. Future studies should address this limitation to enable a more complete and robust assessment of the impact of multi-sensor soil moisture DA by implementing instrumental variable (IV)-based methods for estimating cross-correlated soil moisture errors, which require only two independent soil moisture datasets (Dong et al., 2020).

Domain-averaged vertical profile RMSD metrics of the resulting atmospheric variables show that better specific humidity and air temperature analyses in the lower atmosphere are achieved with single-sensor SMAP DA and ASCAT DA, respectively. Compared to the single-sensor soil moisture DA experiments, assimilating the ASCAT and SMAP soil moisture retrievals together yields balanced performance enhancements, improving both specific humidity and air temperature analyses. Evaluations indicate that soil moisture DA within the KIM-LIS coupled system is particularly effective for the 2 m air temperature analysis and forecast, especially in the multi-sensor soil moisture DA experiment. The synergistic benefits of simultaneously assimilating both soil moisture products are regionally dependent, yielding the greatest advantage when both soil moisture products have a positive impact.

Our experiments demonstrate that, within a land-atmosphere coupled system, soil moisture DA enhances precipitation forecast skill through land–atmosphere interaction processes, particularly when multiple soil moisture products from diverse sources are jointly assimilated. Specifically, multi-sensor soil moisture DA improves the prediction of precipitation events, as evaluated using the ETS metric, across a range of precipitation intensity thresholds.

This study suggests that simultaneously assimilating the ASCAT and SMAP soil moisture products within the KIM-LIS coupled system can leverage their complementary advantages, as demonstrated for the estimates of specific humidity, air temperature, and precipitation. The findings obtained in this study are promising for three main reasons. First, clear synergistic regional skill improvements from multi-sensor DA are evident, particularly in regions and periods where both single-sensor experiments show positive impacts. Second, the magnitude of atmospheric forecast skill improvements from both single- and multi-sensor soil moisture DA, relative to the control experiment (without soil moisture DA), is comparable to improvements reported in previous studies (e.g., Draper and Reichle, 2019; Lin and Pu, 2019; Muñoz-Sabater et al., 2019; Reichle et al., 2023), with multi-sensor DA yielding slightly better (though not statistically significant) performance. Achieving consistent improvements across the globe remains challenging due to factors discussed in Sect. 8, which can cause local skill degradations in atmospheric estimates. Finally, as emphasized above, simultaneous assimilation of ASCAT and SMAP produces

a more balanced improvement across atmospheric variables than single-sensor DA. These results highlight the value of assimilating soil moisture observations from multiple sensors, even if trade-offs remain for certain variables in regions or periods where single-sensor impacts conflict.

To conclude, a key aspect of this study is the joint assimilation of individual radar- and radiometer-based soil moisture products (multi-sensor DA) within a land-atmosphere coupled system to improve weather forecast skill. Compared to assimilating pre-blended soil moisture data, this approach is advantageous because (1) it accounts for the relative uncertainties of both sensors, which vary across space and time; (2) it provides a flexible framework for incorporating various combinations of soil moisture data sources within DA systems; and (3) it is more suitable for near-real time operational forecast systems, the focus of this study, since soil moisture data blending processes may increase latency and thereby reduce data availability for operational use. However, a direct comparison of soil moisture DA performance between the two approaches (i.e., joint assimilation of multiple products and assimilation of a pre-blended product) has not been conducted in this study. It is also acknowledged that the overall domain-averaged improvements in atmospheric estimates achieved through multi-sensor soil moisture DA, relative to single-sensor DA, are limited and statistically insignificant.

The following issues remain to be addressed in future studies to enhance future performance. First, the impact of subsurface scattering on the quality of the ASCAT soil moisture product under dry soil conditions needs to be considered in quality control procedures. Second, an alternative soil moisture bias correction method, especially for ASCAT data, should be explored. Third, more realistic spatially or spatiotemporally distributed estimates of soil moisture observation errors are required to maximize the benefits of multi-sensor soil moisture DA. Lastly, as discussed in several previous studies, addressing biases in the soil moisture-latent heat flux coupling in LSMs (Crow et al., 2023; Kwon et al., 2024; Lei et al., 2018), accounting for the background error covariance between atmospheric and land variables during DA (Kwon et al., 2024), and assimilating screen-level observations (de Rosnay et al., 2013; Lin and Pu, 2020) can improve the positive impacts of soil moisture DA on atmospheric forecasts in coupled systems.

## Appendix A: Abbreviations

| | |
|---|---|
| AMSR2 | Advanced Microwave Scanning Radiometer 2 |
| AMSU-A | Advanced Microwave Sounding Unit-A |
| AMVs | Atmospheric Motion Vectors |
| ASCAT | Advanced SCATterometer |
| ATMS | Advanced Technology Microwave Sounder |
| CDF | Cumulative distribution function |
| CDR | Climate Data Record |
| CPC | Climate Prediction Center |
| CrIS | Cross-track Infrared Sounder |
| CTL | Control case serving as a baseline experiment |
| DA | Data assimilation |
| DCA | Dual Channel Algorithm |
| EASE | Equal Area Scalable Earth |
| ECMWF | European Centre for Medium-Range Weather Forecasts |
| EnKF | Ensemble Kalman filter |
| ERA5 | Fifth generation of the ECMWF atmospheric reanalysis |
| ESA CCI | European Space Agency Climate Change Initiative |
| ESME | Estimated Soil Moisture Error |
| ETS | Equitable threat score |
| EUMETSAT | European Organisation for the Exploitation of Meteorological Satellites |
| FAO | Food and Agriculture Organization |
| FB | Frequency bias |
| fMSE | Fractional mean-square error |
| GLDAS | Global Land Data Assimilation System |
| GPS-RO | Global Positioning System Radio Occultation |
| Hybrid 4DEnVar | Hybrid four-dimensional ensemble variational |
| IASI | Infrared Atmosphere Sounding Interferometer |
| IFS | Integrated Forecasting System |
| IGBP | International Geosphere-Biosphere Programme |
| KIAPS | Korea Institute of Atmospheric Prediction Systems |
| KIM | Korean Integrated Model |
| KPOP | KIM Package of Observation Processing |
| KVAR | KIM VARiational data assimilation |
| LETKF | Local ensemble transform Kalman filter |
| LIS | Land Information System |
| LPRM | Land Parameter Retrieval Model |
| LSM | Land surface model |
| LST | Local solar time |
| L2 | Level 2 |
| MetOp | Meteorological Operational |
| MHS | Microwave Humidity Sounder |
| MODIS | Moderate resolution imaging spectroradiometer |
| MT_ATSP | Multi-sensor soil moisture data assimilation experiment |
| NASA | National Aeronautics and Space Administration |
| NCEP | National Centers for Environmental Prediction |
| NOAA | National Oceanic and Atmospheric Administration |
| NSIDC | National Snow and Ice Data Center |
| NWP | Numerical weather prediction |
| RFI | Radio Frequency Interference |
| RMSD | Root mean square difference |
| SG_AT | Single-sensor data assimilation experiment using the ASCAT soil moisture data |
| SG_SP | Single-sensor data assimilation experiment using the SMAP soil moisture data |
| SMAP | Soil Moisture Active Passive |
| SMOS | Soil Moisture and Ocean Salinity |
| SMOS-IC | SMOS-INRA-CESBIO |
| SRTM | Shuttle Radar Topography Mission |
| STATSGO | State Soil Geographic |
| TCA | Triple collocation analysis |
| TU Wien | Vienna University of Technology |
| UTC | Coordinated Universal Time |
| VV | Vertical transmit vertical receive |
| WMO | World Meteorological Organization |
| 4DIAU | Four-dimensional incremental analysis update |

*Code and data availability.* The NASA Land Information System (LIS) framework is publicly available at https://github.com/NASA-LIS/LISF (last access: 23 February 2026, Kumar et al., 2006). Satellite-based soil moisture data assimilated in this study, i.e., Soil Moisture Active Passive (SMAP) and Advanced SCATterometer (ASCAT), can be obtained from https://doi.org/10.5067/K7Y2D8QQVZ4L (O'Neill et al., 2023) and https://data.eumetsat.int/product/EO:EUM:DAT:METOP:SOMO12 (last access: 23 February 2026), respectively. Other global soil moisture products, used as TCA triplet components to evaluate soil moisture estimates, can be downloaded from https://www.earthdata.nasa.gov/sensors/amsr2 (last access: 23 February 2026) for the Advanced Microwave Scanning Radiometer 2 (AMSR2) and https://www.catds.fr/Products/Products-over-Land/SMOS-IC (last access: 23 February 2026) for the Soil Moisture and Ocean Salinity (SMOS) mission. Integrated Forecasting System (IFS) analysis data can be obtained from the European Centre for Medium-Range Weather Forecasts (ECMWF) in accordance with their data policy. The National Oceanic and Atmospheric Administration (NOAA) Climate Prediction Center (CPC) gauge-based global daily precipitation data can be downloaded from https://psl.noaa.gov/data/gridded/data.cpc.globalprecip.html (last access: 23 February 2026). The Korean Integrated Model (KIM) software is not yet publicly available and cannot be distributed due to the Korean government's security policy. All experimental data generated in this work will be available from the authors upon request.

*Supplement.* The supplement related to this article is available online at https://doi.org/10.5194/hess-30-1261-2026-supplement.

*Author contributions.* YK: conceptualization, methodology, investigation, formal analysis, writing (original draft), writing (review and editing). SJ: data curation, methodology, writing (review and editing). HK: data curation, methodology, validation, writing (review and editing). KHS: validation, writing (review and editing). IHK: supervision, methodology, writing (review and editing). EK: validation, writing (review and editing). SC: validation, writing (review and editing).

*Competing interests.* The contact author has declared that none of the authors has any competing interests.

*Disclaimer.* Publisher's note: Copernicus Publications remains neutral with regard to jurisdictional claims made in the text, published maps, institutional affiliations, or any other geographical representation in this paper. The authors bear the ultimate responsibility for providing appropriate place names. Views expressed in the text are those of the authors and do not necessarily reflect the views of the publisher.

*Acknowledgements.* We sincerely thank the scientists of the NASA LIS team for their considerable efforts in developing the LIS framework and making it publicly available. We would also like to express our gratitude to the research teams of ECMWF, ASCAT, SMAP, AMSR2, SMOS, and NOAA CPC for sharing the data used in this study.

*Financial support.* This research has been primarily supported by the Korea Meteorological Administration R&D project "Development of a Next-Generation Data Assimilation System by the Korea Institute of Atmospheric Prediction Systems (KIAPS)" (grant no. KMA2020-02211). Hyunglok Kim has been supported by grants from the National Research Foundation of Korea (NRF), funded by the Korean government (MSIT) (grant nos. RS-2025-24535700 and RS-2025-02363044).

*Review statement.* This paper was edited by Nadia Ursino and reviewed by three anonymous referees.

## References

Al-Yaari, A., Wigneron, J.-P., Dorigo, W., Colliander, A., Pellarin, T., Hahn, S., Mialon, A., Richaume, P., Fernandez-Moran, R., Fan, L., Kerr, Y. H., and De Lannoy, G.: Assessment and inter-comparison of recently developed/reprocessed microwave satellite soil moisture products using ISMN ground-based measurements, Remote Sens. Environ., 224, 289–303, https://doi.org/10.1016/j.rse.2019.02.008, 2019.

Assouline, S.: Infiltration into soils: conceptual approaches and solutions, Water Resour. Res., 49, 1755–1772, https://doi.org/10.1002/wrcr.20155, 2013.

Azimi, S., Dariane, A. B., Modanesi, S., Bauer-Marschallinger, B., Bindlish, R., Wagner, W., and Massari, C.: Assimilation of Sentinel 1 and SMAP – based satellite soil moisture retrievals into SWAT hydrological model: the impact of satellite revisit time and product spatial resolution on flood simulations in small basins, J. Hydrol., 581, 124367, https://doi.org/10.1016/j.jhydrol.2019.124367, 2020.

Bartalis, Z., Wagner, W., Naeimi, V., Hasenauer, S., Scipal, K., Bonekamp, H., Figa, J., and Anderson, C.: Initial soil moisture retrievals from the METOP-A Advanced Scatterometer (ASCAT), Geophys. Res. Lett., 34, L20401, https://doi.org/10.1029/2007GL031088, 2007.

Baugh, C., de Rosnay, P., Lawrence, H., Jurlina, T., Drusch, M., Zsoter, E., and Prudhomme, C.: The impact of SMOS soil moisture data assimilation within the operational Global Flood Awareness System (GloFAS), Remote Sens., 12, 1490, https://doi.org/10.3390/rs12091490, 2020.

Beljaars, A. C. M., Viterbo, P., Miller, M. J., and Betts, A. K.: The anomalous rainfall over the United States during July1993: Sensitivity to land surface parameterization and soil moisture anomalies, Mon. Weather Rev., 124, 362–383, https://doi.org/10.1175/1520-0493(1996)124<0362:TAROTU>2.0.CO;2, 1996.

Ben Bouallègue, Z., Clare, M. C. A., Magnusson, L., Gascón, E., Maier-Gerber, M., Janoušek, M., Rodwell, M., Pinault, F., Dramsch, J. S., Lang, S. T. K., Raoult, B., Rabier, F., Chevallier, M., Sandu, I., Dueben, P., Chantry, M., and Pappenberger, F.: A first statistical assessment of machine learning-based weather fore-

casts in an operational-like context, B. Am. Meteorol. Soc., 105, E864–E883, https://doi.org/10.1175/BAMS-D-23-0162.1, 2024.

Bhuiyan, H., McNairn, H., Powers, J., Friesen, M., Pacheco, A., Jackson, T. J., Cosh, M. H., Colliander, A., Berg, A., Rowlandson, T., Bullock, P., and Magagi, R.: Assessing SMAP soil moisture scaling and retrieval in the carman (Canada) study site, Vadose Zone J., 17, 180132, https://doi.org/10.2136/vzj2018.07.0132, 2018.

Blyverket, J., Hamer, P. D., Bertino, L., Albergel, C., Fairbairn, D., and Lahoz, W. A.: An evaluation of the EnKF vs. EnOI and the assimilation of SMAP, SMOS and ESA CCI soil moisture data over the contiguous US, Remote Sens., 11, 478, https://doi.org/10.3390/rs11050478, 2019.

Bolten, J. D., Crow, W. T., Zhan, X., Jackson, T. J., and Reynolds, C. A.: Evaluating the utility of remotely sensed soil moisture retrievals for operational agricultural drought monitoring, IEEE J. Sel. Top. Appl. Earth Obs. Remote Sens., 3, 57–66, https://doi.org/10.1109/JSTARS.2009.2037163, 2010.

Bosilovich, M. G. and Sun, W.-Y.: Numerical simulation of the 1993 Midwestern flood: Land–atmosphere interactions, J. Climate, 12, 1490–1505, https://doi.org/10.1175/1520-0442(1999)012<1490:NSOTMF>2.0.CO;2, 1999.

Brocca, L., Melone, F., Moramarco, T., Wagner, W., Naeimi, V., Bartalis, Z., and Hasenauer, S.: Improving runoff prediction through the assimilation of the ASCAT soil moisture product, Hydrol. Earth Syst. Sci., 14, 1881–1893, https://doi.org/10.5194/hess-14-1881-2010, 2010.

Catalano, F., Alessandri, A., De Felice, M., Zhu, Z., and Myneni, R. B.: Observationally based analysis of land–atmosphere coupling, Earth Syst. Dynam., 7, 251–266, https://doi.org/10.5194/esd-7-251-2016, 2016.

Chan, S. K., Bindlish, R., O'Neill, P., Jackson, T., Njoku, E., Dunbar, S., Chaubell, J., Piepmeier, J., Yueh, S., Entekhabi, D., Colliander, A., Chen, F., Cosh, M. H., Caldwell, T., Walker, J., Berg, A., McNairn, H., Thibeault, M., Martínez-Fernández, J., Uldall, F., Seyfried, M., Bosch, D., Starks, P., Holifield Collins, C., Prueger, J., van der Velde, R., Asanuma, J., Palecki, M., Small, E. E., Zreda, M., Calvet, J., Crow, W. T., and Kerr, Y.: Development and assessment of the SMAP enhanced passive soil moisture product, Remote Sens. Environ., 204, 931–941, https://doi.org/10.1016/j.rse.2017.08.025, 2018.

Chaubell, M. J., Yueh, S. H., Dunbar, R. S., Colliander, A., Chen, F., Chan, S. K., Entekhabi, D., Bindlish, R., O'Neill, P. E., Asanuma, J., Berg, A. A., Bosch, D. D., Caldwell, T., Cosh, M. H., Collins, C. H., Martínez-Fernández, J., Seyfried, M., Starks, P. J., Su, Z., Thibeault, M., and Walker, J.: Improved SMAP dual-channel algorithm for the retrieval of soil moisture, IEEE Trans. Geosci. Remote Sens., 58, 3894–3905, https://doi.org/10.1109/tgrs.2019.2959239, 2020.

Chen, M., Shi, W., Xie, P., Silva, V. B. S., Kousky, V. E., Higgins, R. W., and Janowiak, J. E.: Assessing objective techniques for gauge-based analyses of global daily precipitation, J. Geophys. Res., 113, D04110, https://doi.org/10.1029/2007JD009132, 2008.

Cho, E., Kwon, Y., Kumar, S. V., and Vuyovich, C. M.: Assimilation of airborne gamma observations provides utility for snow estimation in forested environments, Hydrol. Earth Syst. Sci., 27, 4039–4056, https://doi.org/10.5194/hess-27-4039-2023, 2023.

Colliander, A., Jackson, T. J., Bindlish, R., Chan, S., Das, N., Kim, S. B., Cosh, M. H., Dunbar, R. S., Dang, L., Pashaian, L., Asanuma, J., Aida, K., Berg, A., Rowlandson, T., Bosch, D., Caldwell, T., Caylor, K., Goodrich, D., al Jassar, H., Lopez-Baeza, E., Martínez-Fernández, J., González-Zamora, A., Livingston, S., McNairn, H., Pacheco, A., Moghaddam, M., Montzka, C., Notarnicola, C., Niedrist, G., Pellarin, T., Prueger, J., Pulliainen, J., Rautiainen, K., Ramos, J., Seyfried, M., Starks, P., Su, Z., Zeng, Y., van der Velde, R., Thibeault, M., Dorigo, W., Vreugdenhil, M., Walker, J. P., Wu, X., Monerris, A., O'Neill, P. E., Entekhabi, D., Njoku, E. G., and Yueh, S.: Validation of SMAP surface soil moisture products with core validation sites, Remote Sens. Environ., 191, 215–231, https://doi.org/10.1016/j.rse.2017.01.021, 2017.

Cook, B. I., Bonan, G. B., and Levis, S.: Soil moisture feedbacks to precipitation in southern Africa, J. Climate, 19, 4198–4206, https://doi.org/10.1175/JCLI3856.1, 2006.

Crow, W. T. and Van den Berg, M. J.: An improved approach for estimating observation and model error parameters in soil moisture data assimilation, Water Resour. Res., 46, W12519, https://doi.org/10.1029/2010WR009402, 2010.

Crow, W. T., Kim, H., and Kumar, S.: Systematic modelling errors undermine the application of land data assimilation systems for hydrological and weather forecasting, J. Hydrometeor., 25, 3–26, https://doi.org/10.1175/JHM-D-23-0069.1, 2023.

Dare, R. A. and Ebert, E. E.: Latitudinal variations in the accuracy of model-generated forecasts of precipitation over Australia and south-east Asia, J. South. Hemisph. Earth Syst. Sci., 67, 46–63, https://doi.org/10.1071/ES17005, 2017.

Das, N. N., Entekhabi, D., Dunbar, R. S., Chaubell, M. J., Colliander, A., Yueh, S., Jagdhuber, T., Chen, F., Crow, W., O'Neill, P. E., Walker, J. P., Berg, A., Bosch, D. D., Caldwell, T., Cosh, M. H., Collins, C. H., Lopez-Baeza, E., and Thibeault, M.: The SMAP and Copernicus Sentinel-1A/B microwave active passive high resolution surface soil moisture product, Remote Sens. Environ., 233, 111380, https://doi.org/10.1016/j.rse.2019.111380, 2019.

Dee, D. P. and Da Silva, A. M.: Data assimilation in the presence of forecast bias, Q. J. Roy. Meteor. Soc., 124, 269–295, https://doi.org/10.1002/qj.49712454512, 1998.

de Rosnay, P., Drusch, M., Vasiljevic, D., Balsamo, G., Albergel, C., and Isaksen, L.: A simplified extended Kalman filter for the global operational soil moisture analysis at ECMWF, Q. J. Roy. Meteor. Soc., 139, 1199–1213, https://doi.org/10.1002/qj.2023, 2013.

de Rosnay, P., Browne, P., de Boisséson, E., Fairbairn, D., Hirahara, Y., Ochi, K., Schepers, D., Weston, P., Zuo, H., Alonso-Balmaseda, M., Balsamo, G., Bonavita, M., Borman, N., Brown, A., Chrust, M., Dahoui, M., Chiara, G., English, S., Geer, A., Healy, S., Hersbach, H., Laloyaux, P., Magnusson, L., Massart, S., McNally, A., Pappenberger, F., and Rabier, F.: Coupled data assimilation at ECMWF: current status, challenges and future developments, Q. J. Roy. Meteor. Soc., 148, 2672–2702, https://doi.org/10.1002/qj.4330, 2022.

Dirmeyer, P. and Halder, S.: Sensitivity of numerical weather forecasts to initial soil moisture variations in CFSv2, Wea. Forecasting, 31, 1973–1983, https://doi.org/10.1175/WAF-D-16-0049.1, 2016.

Dobson, M. C. and Ulaby, F. T.: Active microwave soil moisture research, IEEE Trans. Geosci. Remote Sens., GE-24, 23–36, https://doi.org/10.1109/TGRS.1986.289585, 1986.

Dong, J., Wei, L., Chen, X., Duan, Z., and Lu, Y.: An instrument variable based algorithm for estimating cross-correlated hydrological remote sensing errors, J. Hydrol., 581, 124413, https://doi.org/10.1016/j.jhydrol.2019.124413, 2020.

Dorigo, W. A., Scipal, K., Parinussa, R. M., Liu, Y. Y., Wagner, W., de Jeu, R. A. M., and Naeimi, V.: Error characterisation of global active and passive microwave soil moisture datasets, Hydrol. Earth Syst. Sci., 14, 2605–2616, https://doi.org/10.5194/hess-14-2605-2010, 2010.

Dorigo, W., Wagner, W., Albergel, C., Albrecht, F., Balsamo, G., Brocca, L., Chung, D., Ertl, M., Forkel, M., Gruber, A., Haas, E., Hamer, P. D., Hirschi, M., Ikonen, J., de Jeu, R., Kidd, R., Lahoz, W., Liu, Y. Y., Miralles, D., Mistelbauer, T., Nicolai-Shaw, N., Parinussa, R., Pratola, C., Reimer, C., van der Schalie, R., Seneviratne, S. I., Smolander, T., and Lecomte, P.: ESA CCI soil moisture for improved Earth system understanding: state-of-the art and future directions, Remote Sens. Environ., 203, 185–215, https://doi.org/10.1016/j.rse.2017.07.001, 2017.

Draper, C. and Reichle, R. H.: Assimilation of satellite soil moisture for improved atmospheric reanalyses, Mon. Weather Rev., 147, 2163–2188, https://doi.org/10.1175/MWR-D-18-0393.1, 2019.

Draper, C. S., Mahfouf, J.-F., and Walker, J. P.: Root-zone soil moisture from the assimilation of screen-level variables and remotely sensed soil moisture, J. Geophys. Res., 116, D02127, https://doi.org/10.1029/2010JD013829, 2011.

Draper, C. S., Reichle, R. H., De Lannoy, G. J. M., and Liu, Q.: Assimilation of passive and active microwave soil moisture retrievals, Geophys. Res. Lett., 39, L04401, https://doi.org/10.1029/2011GL050655, 2012.

Draper, C., Reichle, R., de Jeu, R., Naeimi, V., Parinussa, R., and Wagner, W.: Estimating root mean square errors in remotely sensed soil moisture over continental scale domains, Remote Sens. Environ., 137, 288–298, https://doi.org/10.1016/j.rse.2013.06.013, 2013.

Drusch, M. and Viterbo, P.: Assimilation of screen-level variables in ECMWF's Integrated Forecast System: A study on the impact on the forecast quality and analyzed soil moisture, Mon. Weather Rev., 135, 300–314, https://doi.org/10.1175/MWR3309.1, 2007.

ECMWF: IFS Documentation CY43R3 – Part II: Data assimilation. European Centre for Medium-Range Weather Forecasts, Reading, UK, 103 pp., https://doi.org/10.21957/v61kmv92i, 2017.

Ek, M. B., Mitchell, K. E., Lin, Y., Rogers, E., Grunmann, P., Koren, V., Gayno, G., and Tarpley, J. D.: Implementation of Noah land surface model advances in the National Centers for Environmental Prediction operational mesoscale Eta model, J. Geophys. Res., 108, 8851, https://doi.org/10.1029/2002JD003296, 2003.

Entekhabi, D., Njoku, E. G., O'Neill, P. E., Kellogg, K. H., Crow, W. T., and Edelstein, W. N.: The soil moisture active passive (SMAP) mission, Proc. IEEE, 98, 704–716, https://doi.org/10.1109/JPROC.2010.2043918, 2010.

Evensen, G.: Sequential data assimilation with a nonlinear quasi-geostrophic model using Monte Carlo methods to forecast error statistics, J. Geophys. Res., 99, 10143–10162, https://doi.org/10.1029/94JC00572, 1994.

Fairbairn, D., de Rosnay, P., and Weston, P.: Evaluation of an adaptive soil moisture bias correction approach in the ECMWF land data assimilation system, Remote Sens., 16, 493, https://doi.org/10.3390/rs16030493, 2024.

Farr, T. G., Rosen, P. A., Caro, E., Crippen, R., Duren, R., Hensley, S., Kobrick, M., Paller, M., Rodriguez, E., Roth, L., Seal, D., Shaffer, S., Shimada, J., Umland, J., Werner, M., Oskin, M., Burbank, D., and Alsdorf, D.: The shuttle radar topography mission, Rev. Geophys., 45, RG2004, https://doi.org/10.1029/2005RG000183, 2007.

Ferguson, C. R., Agrawal, S., Beauharnois, M. C., Xia, G., Burrows, D. A., and Bosart, L. F.: Assimilation of satellite-derived soil moisture for improved forecasts of the great plains low-level jet, Mon. Weather Rev., 148, 4607–4627, https://doi.org/10.1175/MWR-D-20-0185.1, 2020.

Findell, K. L. and Eltahir, E. A. B.: Atmospheric controls on soil moisture–boundary layer interactions. Part I: Framework development, J. Hydrometeor., 4, 552–569, https://doi.org/10.1175/1525-7541(2003)004<0552:ACOSML>2.0.CO;2, 2003.

Friedl, M. A., McIver, D. K., Hodges, J. C. F., Zhang, X. Y., Muchoney, D., Strahler, A. H., Woodcock, C. E., Gopal, S., Schneider, A., Cooper, A., Baccini, A., Gao, F., and Schaaf, C.: Global land cover mapping from MODIS: algorithms and early results, Remote Sens. Environ., 83, 287–302, https://doi.org/10.1016/S0034-4257(02)00078-0, 2002.

Fuentes, I., Padarian, J., and Vervoort, R. W.: Towards near real-time national-scale soil water content monitoring using data fusion as a downscaling alternative, J. Hydrol., 609, 127705, https://doi.org/10.1016/j.jhydrol.2022.127705, 2022.

Gavahi, K., Abbaszadeh, P., and Moradkhani, H.: How does precipitation data influence the land surface data assimilation for drought monitoring?, Sci. Total Environ., 831, 154916, https://doi.org/10.1016/j.scitotenv.2022.154916, 2022.

Gentine, P., Polcher, J., and Entekhabi, D.: Harmonic propagation of variability in surface energy balance within a coupled soil–vegetation–atmosphere system, Water Resour. Res., 47, W05525, https://doi.org/10.1029/2010WR009268, 2011.

Gruber, A., Su, C.-H., Zwieback, S., Crow, W., Dorigo, W., and Wagner, W.: Recent advances in (soil moisture) triple collocation analysis, Int. J. Appl. Earth Obs., 45, 200–211, https://doi.org/10.1016/j.jag.2015.09.002, 2016.

Hersbach, H., Bell, B., Berrisford, P., Hirahara, S., Horányi, A., Muñoz-Sabater, J., Nicolas, J., Peubey, C., Radu, R., Schepers, D., Simmons, A., Soci, C., Abdalla, S., Abellan, X., Balsamo, G., Bechtold, P., Biavati, G., Bidlot, J., Bonavita, M., De Chiara, G., Dahlgren, P., Dee, D., Diamantakis, M., Dragani, R., Flemming, J., Forbes, R., Fuentes, M., Geer, A., Haimberger, L., Healy, S., Hogan, R. J., Hólm, E., Janisková, M., Keeley, S., Laloyaux, P., Lopez, P., Lupu, C., Radnoti, G., de Rosnay, P., Rozum, I., Vamborg, F., Villaume, S., and Thépaut, J.-N.: The ERA5 global reanalysis, Q. J. Roy. Meteorol. Soc., 146, 1999–2049, https://doi.org/10.1002/qj.3803, 2020.

Hohenegger, C., Brockhaus, P., Bretherton, C. S., and Schär, C.: The soil moisture–precipitation feedback in simulations with explicit and parameterized convection, J. Climate, 22, 5003–5020, https://doi.org/10.1175/2009JCLI2604.1, 2009.

Hong, S.-Y., Kwon, Y. C., Kim, T.-H., Kim, J.-E. E., Choi, S.-J., Kwon, I.-H., Kim, J., Lee, E.-H., Park, R.-S., and Kim, D.-I.: The Korean Integrated Model (KIM) system for global

weather forecasting, Asia-Pac. J. Atmos. Sci., 54, 267–292, https://doi.org/10.1007/s13143-018-0028-9, 2018.

Huang, S., Zhang, X., Chen, N., Ma, H., Fu, P., Dong, J., Gu, X., Nam, W.-H., Xu, L., Rab, G., and Niyogi, D.: A novel fusion method for generating surface soil moisture data with high accuracy, high spatial resolution, and high spatiotemporal continuity, Water Resour. Res., 58, e2021WR030827, https://doi.org/10.1029/2021WR030827, 2022.

Huang, S., Zhang, X., Wang, C., and Chen, N.: Two-step fusion method for generating 1 km seamless multilayer soil moisture with high accuracy in the Qinghai-Tibet plateau, ISPRS J. Photogramm., 197, 346–363, https://doi.org/10.1016/j.isprsjprs.2023.02.009, 2023.

Jalilvand, E., Tajrishy, M., Hashemi, S. A. G. Z., and Brocca, L.: Quantification of irrigation water using remote sensing of soil moisture in a semi-arid region, Remote Sens. Environ., 231, 111226, https://doi.org/10.1016/j.rse.2019.111226, 2019.

Jiang, M., Qiu, T., Wang, T., Zeng, C., Zhang, B., and Shen, H.: Seamless global daily soil moisture mapping using deep learning based spatiotemporal fusion, Int. J. Appl. Earth Obs., 139, 104517, https://doi.org/10.1016/j.jag.2025.104517, 2025.

Jun, S., Park, J.-H., Choi, H.-J., Lee, Y.-H., Lim, Y.-J., Boo, K.-O., and Kang, H.-S.: Impact of soil moisture data assimilation on analysis and medium-range forecasts in an operational global data assimilation and prediction system, Atmosphere, 12, 1089, https://doi.org/10.3390/atmos12091089, 2021.

Kang, J.-H., Chun, H.-W., Lee, S., Ha, J.-H., Song, H.-J., Kwon, I.-H., Han, H.-J., Jeong, H., Kwon, H.-N., and Kim, T.-H.: Development of an observation processing package for data assimilation in KIAPS, Asia-Pac. J. Atmos. Sci., 54, 303–318, https://doi.org/10.1007/s13143-018-0030-2, 2019.

Keppenne, C. L.: Data assimilation into a primitive-equation model with a parallel ensemble Kalman filter, Mon. Weather Rev., 128, 1971–1981, https://doi.org/10.1175/1520-0493(2000)128<1971:DAIAPE>2.0.CO;2, 2000.

Kerr, Y. H., Waldteufel, P., Richaume, P., Wigneron, J. P., Ferrazzoli, P., Mahmoodi, A., Al Bitar, A., Cabot, F., Gruhier, C., Juglea, S. E., Leroux, D., Mialon, A., and Delwart, S.: The SMOS soil moisture retrieval algorithm, IEEE Trans. Geosci. Remote Sens., 50, 1384–1403, https://doi.org/10.1109/TGRS.2012.2184548, 2012.

Khaki, M. and Awange, J.: The application of multi-mission satellite data assimilation for studying water storage changes over South America, Sci. Total Environ., 647, 1557–1572, https://doi.org/10.1016/j.scitotenv.2018.08.079, 2019.

Khaki, M., Hoteit, I., Kuhn, M., Forootan, E., and Awange, J.: Assessing data assimilation frameworks for using multi-mission satellite products in a hydrological context, Sci. Total Environ., 647, 1031–1043, https://doi.org/10.1016/j.scitotenv.2018.08.032, 2019.

Khaki, M., Hendricks Franssen, H.-J., and Han, S. C.: Multi-mission satellite remote sensing data for improving land hydrological models via data assimilation, Sci. Rep., 10, 18791, https://doi.org/10.1038/s41598-020-75710-5, 2020.

Kim, H., Parinussa, R., Konings, A. G., Wagner, W., Cosh, M. H., Lakshmi, V., Zohaib, M., and Choi, M.: Global-scale assessment and combination of SMAP with ASCAT (active) and AMSR2 (passive) soil moisture products, Remote Sens. Environ., 204, 260–275, https://doi.org/10.1016/j.rse.2017.10.026, 2018.

Kim, H., Wigneron, J.-P., Kumar, S., Dong, J., Wagner, W., Cosh, M. H., Bosch, D. D., Collins, C. H., Starks, P. J., Seyfried, M., and Lakshmi, V.: Global scale error assessments of soil moisture estimates from microwave-based active and passive satellites and land surface models over forest and mixed irrigated/dryland agriculture regions, Remote Sens. Environ., 251, 112052, https://doi.org/10.1016/j.rse.2020.112052, 2020.

Kim, H., Lakshmi, V., Kwon, Y., and Kumar, S. V.: First attempt of global-scale assimilation of subdaily scale soil moisture estimates from CYGNSS and SMAP into a land surface model, Environ. Res. Lett., 16, 074041, https://doi.org/10.1088/1748-9326/ac0ddf, 2021a.

Kim, H., Lee, S., Cosh, M. H., Lakshmi, V., Kwon, Y., and McCarty, G. W.: Assessment and combination of SMAP and Sentinel-1A/B-derived soil moisture estimates with land surface model outputs in the Mid-Atlantic Costal Plain, USA, IEEE Trans. Geosci. Remote Sens., 59, 991–1011, https://doi.org/10.1109/TGRS.2020.2991665, 2021b.

Kim, H., Crow, W., Li, X., Wagner, W., Hahn, S., and Lakshmi, V.: True global error maps for SMAP, SMOS, and ASCAT soil moisture data based on machine learning and triple collocation analysis, Remote Sens. Environ., 298, 113776, https://doi.org/10.1016/j.rse.2023.113776, 2023.

Kim, S., Kim, H., Kwon, Y., and Nguyen, H. H.: A standalone framework for predicting spatiotemporal errors in satellite-based soil moisture using tree-based models and deep neural networks, Gisci. Remote Sens., 62, 2475572, https://doi.org/10.1080/15481603.2025.2475572, 2025.

Kolassa, J., Reichle, R. H., and Draper, C. S.: Merging active and passive microwave observations in soil moisture data assimilation, Remote Sens. Environ., 191, 117–130, https://doi.org/10.1016/j.rse.2017.01.015, 2017.

Koo, M.-S., Baek, S., Seol, K.-H., and Cho, K.: Advances in land modeling of KIAPS based on the Noah land surface model, Asia-Pac. J. Atmos. Sci., 53, 361–373, https://doi.org/10.1007/s13143-017-0043-2, 2017.

Koster, R. D., Dirmeyer, P. A., Guo, Z., Bonan, G., Chan, E., Cox, P., Gordon, C. T., Kanae, S., Kowalczyk, E., Lawrence, D., Liu, P., Lu, C.-H., Malyshev, S., Mcavaney, B., Mitchell, K., Mocko, D., Oki, T., Oleson, K., Pitman, A., Sud, Y. C., Taylor, C. M., Verseghy, D., Vasic, R., Xue, Y., and Yamada, T.: Regions of strong coupling between soil moisture and precipitation, Science, 305, 1138–1140, https://doi.org/10.1126/science.1100217, 2004.

Koster, R. D., Guo, Z., Yang, R., Dirmeyer, P. A., Mitchell, K., and Puma, M. J.: On the nature of soil moisture in land surface models, J. Clim., 22, 4322–4335, https://doi.org/10.1175/2009JCLI2832.1, 2009.

Koster, R. D., Mahanama, S. P. P., Yamada, T. J., Balsamo, G., Berg, A. A., Boisserie, M., Dirmeyer, P. A., Doblas-Reyes, F. J., Drewitt, G., Gordon, C. T., Guo, Z., Jeong, J.-H., Lawrence, D. M., Lee, W.-S., Li, Z., Luo, L., Malyshev, S., Merryfield, W. J., Seneviratne, S. I., Stanelle, T., van den Hurk, B. J. J. M., Vitart, F., and Wood, E. F.: Contribution of land surface initialization to subseasonal forecast skill: first results from a multi-model experiment, Geophys. Res. Lett., 37, L02402, https://doi.org/10.1029/2009GL041677, 2010.

Kumar, S. V., Peters-Lidard, C. D., Tian, Y., Houser, P. R., Geiger, J., Olden, S., Lighty, L., Eastman, J. L., Dotu, B., Dirmeyer, P., Adams, J., Mitchell, K., Wood, E. F., and Sheffield, J.: Land in-

formation system: an interoperable framework for high resolution land surface modeling, Environ. Modell. Softw., 21, 1402–1415, https://doi.org/10.1016/j.envsoft.2005.07.004, 2006.

Kumar, S. V., Reichle, R. H., Peters-Lidard, C. D., Koster, R. D., Zhan, X., Crow, W. T., Eylander, J. B., and Houser, P. R.: A land surface data assimilation framework using the land information system: Description and applications, Adv. Water Resour., 31, 1419–1432, https://doi.org/10.1016/j.advwatres.2008.01.013, 2008a.

Kumar, S., Peters-Lidard, C., Tian, Y., Reichle, R. H., Geiger, J., Alonge, C., Eylander, J., and Houser, P.: An integrated hydrologic modeling and data assimilation framework, Computer, 41, 52–59, https://doi.org/10.1109/MC.2008.475, 2008b.

Kumar, S. V., Reichle, R. H., Koster, R. D., Crow, W. T., and Peters-Lidard, C. D.: Role of subsurface physics in the assimilation of surface soil moisture observations, J. Hydrometeorol., 10, 1534–1547, https://doi.org/10.1175/2009JHM1134.1, 2009.

Kumar, S. V., Peters-Lidard, C. D., Mocko, D., Reichle, R., Liu, Y., Arsenault, K. R., Xia, Y., Ek, M., Riggs, G., Livneh, B., and Cosh, M.: Assimilation of remotely sensed soil moisture and snow depth retrievals for drought estimation, J. Hydrometeor., 15, 2446–2469, https://doi.org/10.1175/JHM-D-13-0132.1, 2014.

Kumar, S. V., Peters-Lidard, C. D., Santanello, J. A., Reichle, R. H., Draper, C. S., Koster, R. D., Nearing, G., and Jasinski, M. F.: Evaluating the utility of satellite soil moisture retrievals over irrigated areas and the ability of land data assimilation methods to correct for unmodeled processes, Hydrol. Earth Syst. Sci., 19, 4463–4478, https://doi.org/10.5194/hess-19-4463-2015, 2015.

Kumar, S. V., Dong, J., Peters-Lidard, C. D., Mocko, D., and Gómez, B.: Role of forcing uncertainty and background model error characterization in snow data assimilation, Hydrol. Earth Syst. Sci., 21, 2637–2647, https://doi.org/10.5194/hess-21-2637-2017, 2017.

Kumar, S. V., Dirmeyer, P. A., Peters-Lidard, C. D., Bindlish, R., and Bolten, J.: Information theoretic evaluation of satellite soil moisture retrievals, Remote Sens. Environ., 204, 392–400, https://doi.org/10.1016/j.rse.2017.10.016, 2018.

Kumar, S. V., Jasinski, M., Mocko, D. M., Rodell, M., Borak, J., Li, B., Beaudoing, H. K., and Peters-Lidard, C. D.: NCA-LDAS land analysis: Development and performance of a multisensory, multivariate land data assimilation system for the national climate assessment, J. Hydrometeorol., 20, 1571–1593, https://doi.org/10.1175/JHM-D-17-0125.1, 2019.

Kwon, I.-H., Song, H.-J., Ha, J.-H., Chun, H.-W., Kang, J.-H., Lee, S., Lim, S., Jo, Y., Han, H.-J., Jeong, H., Kwon, H.-N., Shin, S., and Kim, T.-H.: Development of an operational hybrid data assimilation system at KIAPS, Asia-Pac. J. Atmos. Sci., 54, 319–335, https://doi.org/10.1007/s13143-018-0029-8, 2018.

Kwon, Y., Forman, B. A., Ahmad, J. A., Kumar, S. V., and Yoon, Y.: Exploring the utility of machine learning-based passive microwave brightness temperature data assimilation over terrestrial snow in High Mountain Asia, Remote Sens., 11, 2265, https://doi.org/10.3390/rs11192265, 2019.

Kwon, Y., Yoon, Y., Forman, B. A., Kumar, S. V., and Wang, L.: Quantifying the observational requirements of a space-borne LiDAR snow mission, J. Hydrol., 601, 126709, https://doi.org/10.1016/j.jhydrol.2021.126709, 2021.

Kwon, Y., Kumar, S. V., Navari, M., Mocko, D. M., Kemp, E. M., Wegiel, J. W., Geiger, J. V., and Bindlish, R.: Irrigation characterization improved by the direct use of SMAP soil moisture anomalies within a data assimilation system, Environ. Res. Lett., 17, 084006, https://doi.org/10.1088/1748-9326/ac7f49, 2022.

Kwon, Y., Jun, S., Kim, E., Seol, K.-H., Hong, S., Kwon, I.-H., Kang, J.-H., and Kim, H.: Improving weather forecast skill of the Korean Integrated Model by assimilating Soil Moisture Active Passive soil moisture anomalies, Q. J. Roy. Meteor. Soc., 150, 5305–5336, https://doi.org/10.1002/qj.4871, 2024.

Laiolo, P., Gabellani, S., Campo, L., Silvestro, F., Delogu, F., Rudari, R., Pulvirenti, L., Boni, G., Fascetti, F., Pierdicca, N., Crapolicchio, R., Hasenauer, S., and Puca, S.: Impact of different satellite soil moisture products on the predictions of a continuous distributed hydrological model, Int. J. Appl. Earth Obs., 48, 131–145, https://doi.org/10.1016/j.jag.2015.06.002, 2016.

Lamichhane, M., Mehan, S., and Mankin, K. R.: Surface soil moisture prediction using multimodal remote sensing data fusion and machine learning algorithms in semi-arid agricultural region, Sci. Remote Sens., 12, 100255, https://doi.org/10.1016/j.srs.2025.100255, 2025.

Lee, S., Song, H.-J., Chun, H.-W., Kwon, I.-H., Kang, J.-H., and Lim, S.: All-sky microwave humidity sounder assimilation in the Korean Integrated Model forecast system, Q. J. Roy. Meteor. Soc., 146, 3570-3586, https://doi.org/10.1002/qj.3862, 2020.

Lei, F., Crow, W. T., Holmes, T. R. H., Hain, C., and Anderson, M. C.: Global investigation of soil moisture and latent heat flux coupling strength, Water Resour. Res., 54, 8196–8215, https://doi.org/10.1029/2018WR023469, 2018.

Li, S., Zhang, L., Ma, R., Yan, M., and Tian, X.: Improved ET assimilation through incorporating SMAP soil moisture observations using a coupled process model: A study of U.S. arid and semiarid regions, J. Hydrol., 590, 125402, https://doi.org/10.1016/j.jhydrol.2020.125402, 2020.

Lievens, H., De Lannoy, G. J. M., Al Bitar, A., Drusch, M., Dumedah, G., Hendricks Franssen, H.-J., Kerr, Y. H., Tomer, S. K., Martens, B., Merlin, O., Pan, M., Roundy, J. K., Vereecken, H., Walker, J. P., Wood, E. F., Verhoest, N. E. C., and Pauwels, V. R. N.: Assimilation of SMOS soil moisture and brightness temperature products into a land surface model, Remote Sens. Environ., 180, 292–304, https://doi.org/10.1016/j.rse.2015.10.033, 2016.

Lin, X., Huang, S., Li, J., Huang, Q., Shi, H., She, D., Leng, G., Wei, X., Guo, W., Liu, Y., and Luo, J.: Feedback dynamics between precipitation, temperature, and soil moisture in China and their possible driving mechanisms under a changing environment, Atmos. Res., 294, 106983, https://doi.org/10.1016/j.atmosres.2023.106983, 2023.

Lin, L.-F. and Pu, Z.: Examining the impact of SMAP soil moisture retrievals on short-range weather prediction under weakly and strongly coupled data assimilation with WRF-Noah, Mon. Weather Rev., 147, 4345–4366, https://doi.org/10.1175/MWR-D-19-0017.1, 2019.

Lin, L.-F. and Pu, Z.: Improving near-surface short-range weather forecasts using strongly coupled land–atmosphere data assimilation with GSI-EnKF, Mon. Weather Rev., 148, 2863–2888, https://doi.org/10.1175/MWR-D-19-0370.1, 2020.

Liu, Q., Reichle, R. H., Bindlish, R., Cosh, M. H., Crow, W. T., de Jeu, R., De Lannoy, G. J. M., Huffman, G. J., and Jack-

son, T. J.: The contributions of precipitation and soil moisture observations to the skill of soil moisture estimates in a land data assimilation system, J. Hydrometeorol., 12, 750–765, https://doi.org/10.1175/JHM-D-10-05000.1, 2011.

Lodh, A., Routray, A., Dutta, D., George, J. P., and Mitra, A. K.: Improving the prediction of monsoon depressions by assimilating ASCAT soil moisture in NCUM-R modeling system, Atmos. Res., 272, 106130, https://doi.org/10.1016/j.atmosres.2022.106130, 2022.

Long, D., Bai, L., Yan, L., Zhang, C., Yang, W., Lei, H., Quan, J., Meng, X., and Shi, C.: Generation of spatially complete and daily continuous surface soil moisture of high spatial resolution, Remote Sens. Environ., 233, 111364, https://doi.org/10.1016/j.rse.2019.111364, 2019.

Lorenc, A. C., Bowler, N. E., Clayton, A. M., Pring, S. R., and Fairbairn, D.: Comparison of hybrid-4DEnVar and hybrid-4DVar data assimilation methods for global NWP, Mon. Weather Rev., 143, 212–229, https://doi.org/10.1175/MWR-D-14-00195.1, 2015.

Miller, D. A. and White, R. A.: A conterminous United States multilayer soil characteristics dataset for regional climate and hydrology modelling, Earth Interact., 2, 1–26, https://doi.org/10.1175/1087-3562(1998)002<0001:ACUSMS>2.3.CO;2, 1998.

Min, X., Shangguan, Y., Li, D., and Shi, Z.: Improving the fusion of global soil moisture datasets from SMAP, SMOS, ASCAT, and MERRA2 by considering the non-zero error covariance, Int. J. Appl. Earth Obs., 113, 103016, https://doi.org/10.1016/j.jag.2022.103016, 2022.

Muñoz-Sabater, J., Lawrence, H., Albergel, C., de Rosnay, P., Isaksen, L., Mecklenburg, S., Kerr, Y., and Drusch, M.: Assimilation of SMOS brightness temperatures in the ECMWF integrated forecasting system, Q. J. Roy. Meteor. Soc., 145, 2524–2548, https://doi.org/10.1002/QJ.3577, 2019.

Nair, A. S. and Indu, J.: A coupled land surface and radiative transfer models based on relief correction for a reliable land data assimilation over mountainous terrain, IEEE Geosci. Remote Sens. Lett., 15, 1657–1661, https://doi.org/10.1109/LGRS.2018.2854908, 2018.

Nair, A. S. and Indu, J.: Improvement of land surface model simulations over India via data assimilation of satellite-based soil moisture products, J. Hydrol., 573, 406–421, https://doi.org/10.1016/j.jhydrol.2019.03.088, 2019.

Nearing, G., Yatheendradas, S., Crow, W., Zhan, X., Liu, J., and Chen, F.: The efficiency of data assimilation, Water Resour. Res., 54, 6374–6392, https://doi.org/10.1029/2017WR020991, 2018.

Nguyen, H. H., Kim, H., Crow, W., Yueh, S., Wagner, W., Lei, F., Wigneron, J.-P., Colliander, A., and Frappart, F.: From theory to hydrological practice: Leveraging CYGNSS data over seven years for advanced soil moisture monitoring, Remote Sens. Environ., 316, 114509, https://doi.org/10.1016/j.rse.2024.114509, 2025.

O'Neill, P. E., Chan, S., Njoku, E. G., Jackson, T., Bindlish, R. and Chaubell, J.: SMAP L2 Radiometer Half-Orbit 36 km EASE-Grid Soil Moisture, SPL2SMP, Version 9, NASA National Snow and Ice Data Center Distributed Active Archive Center [data set], https://doi.org/10.5067/K7Y2D8QQVZ4L, 2023.

Orth, R. and Seneviratne, S. I.: Propagation of soil moisture memory to streamflow and evapotranspiration in Europe, Hydrol. Earth Syst. Sci., 17, 3895–3911, https://doi.org/10.5194/hess-17-3895-2013, 2013.

Pal, J. S. and Eltahir, E. A. B.: A feedback mechanism between soil-moisture distribution and storm tracks, Q. J. Roy. Meteor. Soc., 129, 2279–2297, https://doi.org/10.1256/qj.01.201, 2003.

Paloscia, S. and Pampaloni, P.: Microwave polarization index for monitoring vegetation growth, IEEE Trans. Geosci. Remote Sens., 26, 617–621, https://doi.org/10.1109/36.7687, 1988.

Peters-Lidard, C. D., Houser, P. R., Tian, Y., Kumar, S. V., Geiger, J., Olden, S., Lighty, L., Doty, B., Dirmeyer, P., Adams, J., Mitchell, K., Wood, E. F., and Sheffield, J.: High-performance Earth system modeling with NASA/GSFC's land information system, Innov. Syst. Softw. Eng., 3, 157–165, https://doi.org/10.1007/s11334-007-0028-x, 2007.

Pipunic, R. C., Walker, J. P., Western, A. W., and Trudinger, C. M.: Assimilation of multiple data types for improved heat flux prediction: a one-dimensional field study, Remote Sens. Environ., 136, 315–329, https://doi.org/10.1016/j.rse.2013.05.015, 2013.

Polichtchouk, I., van Niekerk, A., and Wedi, N.: Resolved gravity waves in the extratropical stratosphere: Effect of horizontal resolution increase from $O(10)$ to $O(1)$ km, J. Atmos. Sci., 80, 473–486, https://doi.org/10.1175/JAS-D-22-0138.1, 2023.

Reichle, R. H. and Koster, R. D.: Bias reduction in short records of satellite soil moisture, Geophys. Res. Lett., 31, L19501, https://doi.org/10.1029/2004GL020938, 2004.

Reichle, R. H., McLaughlin, D. B., and Entekhabi, D.: Hydrologic data assimilation with the ensemble Kalman filter, Mon. Weather Rev., 130, 103–114, https://doi.org/10.1175/1520-0493(2002)130<0103:HDAWTE>2.0.CO;2, 2002a.

Reichle, R. H., Walker, J. P., Koster, R. D., and Houser, P. R.: Extended versus ensemble Kalman filtering for land data assimilation, J. Hydrometeorol., 3, 728–740, https://doi.org/10.1175/1525-7541(2002)003<0728:EVEKFF>2.0.CO;2, 2002b.

Reichle, R. H., Koster, R. D., Liu, P., Mahanama, S. P. P., Njoku, E. G., and Owe, M.: Comparison and assimilation of global soil moisture retrievals from the advanced microwave scanning radiometer for the earth observing system (AMSR-E) and the scanning multichannel microwave radiometer (SMMR), J. Geophys. Res. Atmos., 112, D09108, https://doi.org/10.1029/2006JD008033, 2007.

Reichle, R. H., Crow, W. T., Koster, R. D., Sharif, H. O., and Mahanama, S. P. P.: Contribution of soil moisture retrievals to land data assimilation products, Geophys. Res. Lett., 35, L01404, https://doi.org/10.1029/2007GL031986, 2008.

Reichle, R. H., Zhang, S. Q., Kolassa, J., Liu, Q., and Todling, R.: A weakly-coupled land surface analysis with SMAP radiance assimilation improves GEOS medium-range forecasts of near-surface air temperature and humidity, Q. J. Roy. Meteor. Soc., 149, 1867–1889, https://doi.org/10.1002/qj.4486, 2023.

Renzullo, L. J., van Dijk, A. I. J. M., Perraud, J.-M., Collins, D., Henderson, B., Jin, H., Smith, A. B., and McJannet, D. L.: Continental satellite soil moisture data assimilation improves root-zone moisture analysis for water resources assessment, J. Hydrol., 519, 2747–2762, https://doi.org/10.1016/j.jhydrol.2014.08.008, 2014.

Reynolds, C. A., Jackson, T. J., and Rawls, W. J.: Estimating soil water-holding capacities by linking the Food and Agriculture Organization Soil map of the world with global pedon databases

and continuous pedotransfer functions, Water Resour. Res., 36, 3653–3662, https://doi.org/10.1029/2000WR900130, 2000.

Rodell, M., Houser, P. R., Jambor, U., Gottschalck, J., Mitchell, K., Meng, C.-J., Arsenault, K., Cosgrove, B., Radakovich, J., Bosilovich, M., Entin, J. K., Walker, J. P., Lohmann, D., and Toll, D.: The Global Land Data Assimilation System, Bull. Am. Meteorol. Soc., 85, 381–394, https://doi.org/10.1175/BAMS-85-3-381, 2004.

Santanello Jr., J. A., Kumar, S. V., Peters-Lidard, C. D., and Lawston, P. M.: Impact of soil moisture assimilation on land surface model spinup and coupled land–atmosphere prediction, J. Hydrometeorol., 17, 517–540, https://doi.org/10.1175/JHM-D-15-0072.1, 2016.

Schmugge, T. J., O'Neill, P. E., and Wang, J. R.: Passive microwave soil moisture research, IEEE Trans. Geosci. Remote Sens., GE-24, 1, https://doi.org/10.1109/TGRS.1986.289584, 1986.

Scipal, K., Holmes, T., De Jeu, R., Naeimi, V., and Wagner, W.: A possible solution for the problem of estimating the error structure of global soil moisture data sets, Geophys. Res. Lett., 35, L24403, https://doi.org/10.1029/2008GL035599, 2008.

Seo, E., Lee, M.-I., and Reichle, R. H.: Assimilation of SMAP and ASCAT soil moisture retrievals into the JULES land surface model using the Local Ensemble Transform Kalman Filter, Remote Sens. Environ., 253, 112222, https://doi.org/10.1016/j.rse.2020.112222, 2021.

Shellito, P. J., Small, E. E., and Cosh, M. H.: Calibration of Noah soil hydraulic property parameters using surface soil moisture from SMOS and Basinwide in situ observations, J. Hydrometeorol., 17, 2275–2292, https://doi.org/10.1175/JHM-D-15-0153.1, 2016.

Shellito, P. J., Small, E. E., and Livneh, B.: Controls on surface soil drying rates observed by SMAP and simulated by the Noah land surface model, Hydrol. Earth Syst. Sci., 22, 1649–1663, https://doi.org/10.5194/hess-22-1649-2018, 2018.

Shin, Y. and Jung, Y.: Development of irrigation water management model for reducing drought severity using remotely sensed soil moisture footprints, J. Irrig. Drain. Eng., 140, 04014021, https://doi.org/10.1061/(ASCE)IR.1943-4774.0000736, 2014.

Singh, A. and Gaurav, K.: Deep learning and data fusion to estimate surface soil moisture from multi-sensor satellite images, Sci. Rep., 13, 2251, https://doi.org/10.1038/s41598-023-28939-9, 2023.

Song, H.-J., Shin, S., Ha, J.-H., and Lim, S.: The advantages of hybrid 4DEnVar in the context of the forecast sensitivity to initial conditions, J. Geophys. Res. Atmos., 122, 12226–12244, https://doi.org/10.1002/2017JD027598, 2017.

Stoffelen, A.: Toward the true near-surface wind speed: error modeling and calibration using triple collocation, J. Geophys. Res., 103, 7755–7766, https://doi.org/10.1029/97JC03180, 1998.

Tangdamrongsub, N., Han, S.-C., Yeo, I.-Y., Dong, J., Steele-Dunne, S. C., Willgoose, G., and Walker, J. P.: Multivariate data assimilation of GRACE, SMOS, SMAP measurements for improved regional soil moisture and groundwater storage estimates, Adv. Water Resour., 135, 103477, https://doi.org/10.1016/j.advwatres.2019.103477, 2020.

Tuttle, S. and Salvucci, G.: Empirical evidence of contrasting soil moisture–precipitation feedbacks across the United States, Science, 352, 825–828, https://doi.org/10.1126/science.aaa7185, 2016.

van den Hurk, B., Doblas-Reyes, F., Balsamo, G., Koster, R. D., Seneviratne, S. I., and Camargo Jr., H.: Soil moisture effects on seasonal temperature and precipitation forecast scores in Europe, Climate Dyn., 38, 349–362, https://doi.org/10.1007/s00382-010-0956-2, 2012.

van der Schalie, R., de Jeu, R., Rodríguez-Fernández, N., Al-Yaari, A., Kerr, Y., Wigneron, J.-P., Parinussa, R., and Drusch, M.: The Effect of three different data fusion approaches on the quality of soil moisture retrievals from multiple passive microwave sensors, Remote Sens., 10, 107, https://doi.org/10.3390/rs10010107, 2018.

Wagner, W., Lemoine, G., and Rott, H.: A method for estimating soil moisture from ERS scatterometer and soil data, Remote Sens. Environ., 70, 191–207, https://doi.org/10.1016/S0034-4257(99)00036-X, 1999.

Wagner, W., Bartalis, Z., Naeimi, V., Park, S.-E., Figa-Saldaña, J., and Bonekamp, H.: Status of the MetOp ASCAT soil moisture product, IEEE Int. Geosci. Remote. Se. Proceedings, 25–30 July 2010, 276–279, https://doi.org/10.1109/IGARSS.2010.5653358, 2010.

Wagner, W., Hahn, S., Kidd, R., Melzer, T., Bartalis, Z., Hasenauer, S., Figa-Saldaña, J., De Rosnay, P., Jann, A., Schneider, S., Komma, J., Kubu, G., Brugger, K., Aubrecht, C., Züger, J., Gangkofner, U., Kienberger, S., Brocca, L., Wang, Y., Blöschl, G., Eitzinger, J., Steinnocher, K., Zeil, P., and Rubel, F.: The ASCAT soil moisture product: A review of its specifications, validation results, and emerging applications, Meteorologische Zeitschrift, 22, 5–33, https://doi.org/10.1127/0941-2948/2013/0399, 2013.

Wagner, W., Lindorfer, R., Hahn, S., Kim, H., Vreugdenhil, M., Gruber, A., Fischer, M., and Trnka, M.: Global scale mapping of subsurface scattering signals impacting ASCAT soil moisture retrievals, IEEE Trans. Geosci. Remote Sens., 62, 4509520, https://doi.org/10.1109/TGRS.2024.3429550, 2024.

Wanders, N., Karssenberg, D., de Roo, A., de Jong, S. M., and Bierkens, M. F. P.: The suitability of remotely sensed soil moisture for improving operational flood forecasting, Hydrol. Earth Syst. Sci., 18, 2343–2357, https://doi.org/10.5194/hess-18-2343-2014, 2014.

Wang, Y., Mao, J., Jin, M., Hoffman, F. M., Shi, X., Wullschleger, S. D., and Dai, Y.: Development of observation-based global multilayer soil moisture products for 1970 to 2016, Earth Syst. Sci. Data, 13, 4385–4405, https://doi.org/10.5194/essd-13-4385-2021, 2021.

WMO: Recommendations for the verification and intercomparison of QPFs and PQPFs from operational NWP models, WWRP 2009-1, World Meteorological Organization (WMO), Switzerland, https://wmoomm.sharepoint.com/sites/wmocpdb/ (last access: 23 February 2026), 2008.

Wu, K., Ryu, D., Nie, L., and Shu, H.: Time-variant error characterization of SMAP and ASCAT soil moisture using Triple Collocation Analysis, Remote Sens. Environ., 256, 112324, https://doi.org/10.1016/j.rse.2021.112324, 2021.

Xie, P., Yatagai, A., Chen, M., Hayasaka, T., Fukushima, Y., Liu, C., and Yang, S.: A gauge-based analysis of daily precipitation over East Asia, J. Hydrometeorol., 8, 607–626, https://doi.org/10.1175/JHM583.1, 2007.

Xie, Q., Jia, L., Menenti, M., and Hu, G.: Global soil moisture data fusion by Triple Collocation Analysis from 2011 to 2018, Sci. Data, 9, 687, https://doi.org/10.1038/s41597-022-01772-x, 2022.

Xu, T., Chen, F., He, X., Barlage, M., Zhang, Z., Liu, S., and He, X.: Improve the performance of the Noah-MP-Crop model by jointly assimilating soil moisture and vegetation phenology data, J. Adv. Model. Earth Sy., 13, e2020MS002394, https://doi.org/10.1029/2020MS002394, 2021.

Yang, L., Sun, G., Zhi, L., and Zhao, J.: Negative soil moisture-precipitation feedback in dry and wet regions, Sci. Rep., 8, 4026, https://doi.org/10.1038/s41598-018-22394-7, 2018.

Yin, J., Hain, C. R., Zhan, X., Dong, J., and Ek, M.: Improvements in the forecasts of near-surface variables in the Global Forecast System (GFS) via assimilating ASCAT soil moisture retrievals, J. Hydrol., 578, 124018, https://doi.org/10.1016/j.jhydrol.2019.124018, 2019.

Yuan, X., Wood, E. F., Luo, L., and Pan, M.: A first look at Climate Forecast System version 2 (CFSv2) for hydrological seasonal prediction, Geophys. Res. Lett., 38, L13402, https://doi.org/10.1029/2011GL047792, 2011.

Zhang, H., Wang, S., Liu, K., Li, X., Li, Z., Zhang, X., and Liu, B.: Downscaling of AMSR-E soil moisture over north China using random forest regression, ISPRS Int. J. Geo Inf., 11, 101, https://doi.org/10.3390/ijgi11020101, 2022.

Zeng, J., Yuan, X., and Ji, P.: The important role of reliable land surface model simulation in high-resolution multi-source soil moisture data fusion by machine learning, J. Hydrol., 630, 130700, https://doi.org/10.1016/j.jhydrol.2024.130700, 2024.